

# Improving the Foundation Layers for Concrete Pavements

---

## TECHNICAL REPORT:

## Assessment of Seasonal Variations in Concrete Pavement Foundation Layers – Multiple Test Sections in Iowa



**February 2016**

### Sponsored by

Federal Highway Administration (DTFH 61-06-H-00011 (Work Plan #18))

FHWA TPF-5(183): California, Iowa (lead state), Michigan, Pennsylvania, Wisconsin

---

**National Concrete Pavement  
Technology Center**



CENTER FOR

**CEER**

**EARTHWORKS ENGINEERING  
RESEARCH**

**IOWA STATE UNIVERSITY**  
Institute for Transportation

## **About the National CP Tech Center**

The mission of the National Concrete Pavement Technology (CP Tech) Center is to unite key transportation stakeholders around the central goal of advancing concrete pavement technology through research, tech transfer, and technology implementation.

## **About CEER**

The mission of the Center for Earthworks Engineering Research (CEER) at Iowa State University is to be the nation's premier institution for developing fundamental knowledge of earth mechanics, and creating innovative technologies, sensors, and systems to enable rapid, high quality, environmentally friendly, and economical construction of roadways, aviation runways, railroad embankments, dams, structural foundations, fortifications constructed from earth materials, and related geotechnical applications.

## **Disclaimer Notice**

The contents of this report reflect the views of the authors, who are responsible for the facts and the accuracy of the information presented herein. The opinions, findings and conclusions expressed in this publication are those of the authors and not necessarily those of the sponsors.

The sponsors assume no liability for the contents or use of the information contained in this document. This report does not constitute a standard, specification, or regulation.

The sponsors do not endorse products or manufacturers. Trademarks or manufacturers' names appear in this report only because they are considered essential to the objective of the document.

## **Iowa State University Non-Discrimination Statement**

Iowa State University does not discriminate on the basis of race, color, age, ethnicity, religion, national origin, pregnancy, sexual orientation, gender identity, genetic information, sex, marital status, disability, or status as a U.S. veteran. Inquiries regarding non-discrimination policies may be directed to Office of Equal Opportunity, Title IX/ADA Coordinator, and Affirmative Action Officer, 3350 Beardshear Hall, Ames, Iowa 50011, 515-294-7612, email [eooffice@iastate.edu](mailto:eooffice@iastate.edu).

## **Iowa Department of Transportation Statements**

Federal and state laws prohibit employment and/or public accommodation discrimination on the basis of age, color, creed, disability, gender identity, national origin, pregnancy, race, religion, sex, sexual orientation or veteran's status. If you believe you have been discriminated against, please contact the Iowa Civil Rights Commission at 800-457-4416 or the Iowa Department of Transportation affirmative action officer. If you need accommodations because of a disability to access the Iowa Department of Transportation's services, contact the agency's affirmative action officer at 800-262-0003.

The preparation of this report was financed in part through funds provided by the Iowa Department of Transportation through its "Second Revised Agreement for the Management of Research Conducted by Iowa State University for the Iowa Department of Transportation" and its amendments.

The opinions, findings, and conclusions expressed in this publication are those of the authors and not necessarily those of the Iowa Department of Transportation or the U.S. Department of Transportation Federal Highway Administration.

### Technical Report Documentation Page

<b>1. Report No.</b> DTFH 61-06-H-00011 Work Plan 18	<b>2. Government Accession No.</b>	<b>3. Recipient's Catalog No.</b>	
<b>4. Title and Subtitle</b> Improving the Foundation Layers for Concrete Pavements: Assessment of Seasonal Variations in Concrete Pavement Foundation Layers – Multiple Test Sections in Iowa		<b>5. Report Date</b> February 2016	
		<b>6. Performing Organization Code</b>	
<b>7. Author(s)</b> David J. White, Pavana Vennapusa, Yang Zhang, Alex Johnson		<b>8. Performing Organization Report No.</b> InTrans Project 09-352	
<b>9. Performing Organization Name and Address</b> National Concrete Pavement Technology Center and Center for Earthworks Engineering Research Iowa State University 2711 South Loop Drive, Suite 4700 Ames, IA 50010-8664		<b>10. Work Unit No. (TRAIS)</b>	
		<b>11. Contract or Grant No.</b>	
<b>12. Sponsoring Organization Name and Address</b> Federal Highway Administration U.S. Department of Transportation 1200 New Jersey Avenue SE Washington, DC 20590		<b>13. Type of Report and Period Covered</b> Technical Report	
		<b>14. Sponsoring Agency Code</b> TPF-5(183)	
<b>15. Supplementary Notes</b> Visit <a href="http://www.cptechcenter.org">www.cptechcenter.org</a> or <a href="http://www.ceer.iastate.edu">www.ceer.iastate.edu</a> for color PDF files of this and other research reports.			
<b>16. Abstract</b> <p>This technical project report is one of the field project reports developed as part of the TPF-5(183) and FHWA DTFH 61-06-H-00011:WO18 studies.</p> <p>In cold climates, pavement surfaces and foundation layers are subjected to seasonal temperature variation and freeze-thaw cycles. The number and duration of freeze-thaw cycles in foundation layers can significantly influence pavement performance. Seasonal variation in foundation layers is accounted for in pavement design by empirically adjusting foundation layer moduli values. This paper presents results from in situ falling weight deflectometer (FWD) and dynamic cone penetrometer (DCP) tests conducted over a two-year period at five sites in Iowa; at one of these sites, temperatures of the foundation layers were continuously monitored during the testing period. FWD testing was conducted to determine modulus of subgrade reaction (<math>k</math>) values, and DCP testing was conducted to estimate California bearing ratio (CBR) values of the foundation layers. Temperature data was analyzed to determine freezing and thawing periods and frost penetration in the foundation layers. Seasonal variations observed in the mechanistic properties of the foundation layers were compared with assumed design values, and empirical relationships between the mechanistic properties were explored.</p> <p>For the five sections tested in this study, there were no significant differences in the <math>k</math> values obtained from the FWD in thawed conditions and summer. At four of the five sites, there were no significant differences in the CBR values obtained from DCP tests during thawed and summer conditions. The <math>k</math> values from FWD during frozen conditions were about 10% to 56% higher than in summer at four of the five sites. At one test site, the values were about the same at all testing times. At two of the five sites, <math>k</math> values from FWD were about 1.5 to 2 times lower than the design assumed <math>k</math> value (41 kPa/mm) in thawed condition and in summer. Empirical relationships presented in the design guides to convert CBR to <math>k</math> or <math>M_r</math> to <math>k</math> showed much higher values compared with measured values. Pavement age, <math>k</math> values, and subgrade CBR values were all strongly correlated to the pavement condition index (PCI) values.</p>			
<b>17. Key Words</b> concrete pavement—pavement foundation—mechanistic property—seasonal variation—in situ testing—subgrade		<b>18. Distribution Statement</b> No restrictions.	
<b>19. Security Classification (of this report)</b> Unclassified.	<b>20. Security Classification (of this page)</b> Unclassified.	<b>21. No. of Pages</b> 92	<b>22. Price</b> NA





# **IMPROVING THE FOUNDATION LAYERS FOR CONCRETE PAVEMENTS: ASSESSMENT OF SEASONAL VARIATIONS IN CONCRETE PAVEMENT FOUNDATION LAYERS – MULTIPLE TEST SECTIONS IN IOWA**

**Technical Report**  
February 2016

## **Research Team Members**

Tom Cackler, David J. White, Jeffrey R. Roesler, Barry Christopher, Andrew Dawson,  
Heath Gieselman, and Pavana Vennapusa

## **Report Authors**

David J. White, Pavana K. R. Vennapusa,  
Yang Zhang, Alex Johnson, Heath Gieselman  
Iowa State University

## **Sponsored by**

the Federal Highway Administration (FHWA)  
DTFH61-06-H-00011 Work Plan 18  
FHWA Pooled Fund Study TPF-5(183): California, Iowa (lead state),  
Michigan, Pennsylvania, Wisconsin

**Preparation of this report was financed in part**  
through funds provided by the Iowa Department of Transportation  
through its Research Management Agreement with the  
Institute for Transportation  
(InTrans Project 09-352)

## **National Concrete Pavement Technology Center and Center for Earthworks Engineering Research**

Iowa State University  
2711 South Loop Drive, Suite 4700  
Ames, IA 50010-8664  
Phone: 515-294-8103  
[www.cptechcenter.org](http://www.cptechcenter.org) and [www.ceer.iastate.edu](http://www.ceer.iastate.edu)



## TABLE OF CONTENTS

ACKNOWLEDGMENTS .....	ix
LIST OF SYMBOLS AND ACRONYMS .....	xi
EXECUTIVE SUMMARY .....	xiii
CHAPTER 1. INTRODUCTION .....	1
CHAPTER 2. BACKGROUND .....	3
Seasonal Freeze-Thaw Cycles in Pavements and Foundation Layers .....	3
Seasonal Variations in Pavement Foundation Mechanistic Properties .....	9
Frost Heave .....	9
Thaw Weakening .....	9
CHAPTER 3. EXPERIMENTAL TESTING .....	18
Test Sections .....	18
Kuab Falling Weight Deflectometer .....	23
Dynamic Cone Penetrometer .....	28
Pavement Condition Index.....	29
CHAPTER 4. IN SITU TEST RESULTS .....	31
Seasonal Variations in Mechanistic Properties .....	31
Empirical Relationships between $k$ , $M_r$ , and CBR Values.....	37
Mechanistic Properties versus Pavement Performance .....	38
CHAPTER 5. SUMMARY OF KEY FINDINGS.....	41
REFERENCES .....	43
APPENDIX A: AASHTO (1993) AND PCA (1984) DESIGN CHARTS .....	47
APPENDIX B: FWD TEST RESULTS .....	49
APPENDIX C: DCP TEST RESULTS .....	55
APPENDIX D: PICTURES FROM EACH TEST SITE.....	61

## LIST OF FIGURES

Figure 1. Model of seasonal ground freezing and thawing periods beneath pavement (Andersland and Ladanyi 2004).....	5
Figure 3. Winter 1958-1959: Computed frozen zones (top) and cumulative freeze-thaw cycles (bottom) (Hoover et al. 1962).....	7
Figure 4. Winter 1959-1960: Computed frozen zones (top) and cumulative freeze-thaw cycles (bottom) (Hoover et al. 1962).....	8
Figure 5. Frost penetration plot (Janoo and Berg 1996).....	10
Figure 6. Change in basin area during spring thaw (Janoo and Berg 1996).....	11
Figure 7. Joint transfer efficiency during spring thaw (Janoo and Berg 1996).....	11
Figure 8. Expected seasonal variation of FWD indices (Drumm and Meier 2003).....	13
Figure 9. Frost depth measured with thermocouples, thermistors, and time domain reflectometry probes (Jong et al. 1998).....	14
Figure 10. Changes in seasonal FWD deflection basins (Jong et al. 1998).....	14
Figure 11. Changes in seasonal resilient modulus (Jong et al. 1998).....	15
Figure 12. Typical pavement deflection response due to seasonal changes (Newcomb and Birgisson 1999).....	15
Figure 13. Seasonal changes in the resilient moduli of base and subgrade layers (Newcomb and Birgisson 1999).....	16
Figure 14. Tracking thawing process by using DCP backcalculated moduli (Saarenketo and Saara 2005).....	17
Figure 15. Map showing the in situ test sites.....	20
Figure 16. TS1: US 20 WB near Fort Dodge.....	20
Figure 17. TS2: US 59 NB near Denison.....	21
Figure 18. TS3: US 20 EB near Merville.....	21
Figure 19. TS4: US 30 WB near Nevada (Nevada east).....	22
Figure 20. TS4: US 30 EB near Nevada (Nevada west).....	22
Figure 21. TS5: US 218 SB near Plainfield.....	23
Figure 22. FWD deflection sensor setup used for this study and an example deflection basin.....	24
Figure 23. Void detection using load-deflection data from FWD test.....	25
Figure 24. Static $k_{PLT}$ values versus $k_{FWD-Dynamic}$ measurements reported in literature.....	28
Figure 25. In situ testing procedures: Kuab FWD setup with 300 mm diameter loading plate (a) and DCP with 2m extension rods (b).....	29
Figure 27. $0^{\circ}$ isotherm with time (a), seasonal variations of $D_0$ (b), and seasonal variations of $k_{FWD-Static-Corr}$ (c) at the Plainfield test site.....	32
Figure 28. Number of freeze-thaw cycles versus depth during winter 2010–2011 at US Highway 218 near Plainfield, Iowa.....	33
Figure 29. Seasonal variations in mechanistic properties at the five test sites: $CBR_{SB}$ (a) $CBR_{SG}$ (b), $CBR_{SG-Weak}$ (c), and $k_{FWD-Static-Corr}$ (d).....	34
Figure 30. DCP-CBR profiles at the five test sites in February (frozen state), March (thawed state), and August (summer).....	35
Figure 31. Summary of seasonal changes in $CBR_{SB}$ (a), $CBR_{SG}$ (b), $CBR_{SG-Weak}$ (c), and $k_{FWD-Static-Corr}$ (d) at each site.....	36

Figure 32. Relationship between $M_r$ values determined from CBR and $k_{FWD-Static-Corr}$ compared with the relationship proposed in AASHTO (1993) (left) and relationship between CBR values and $k_{FWD-Static-Corr}$ compared with the relationship proposed in PCA (1984) .....	37
Figure 33. PCI versus pavement age from this study in comparison with results presented in White and Vennapusa (2012) and White et al. (2008) .....	39
Figure 34. PCI versus $k_{FWD-Static-Corr}$ (left) and $CBR_{SG-Weak}$ (right).....	40
Figure 35. Chart for estimating resilient modulus ( $M_r$ ) of subgrade from CBR (from AASHTO 1993 Appendix FF based on results from Til et al. 1972) .....	47
Figure 36. Chart for estimating modulus of subgrade reaction ( $k$ ) from CBR (from PCA 1984) .....	48
Figure 37. Seasonal FWD test results of US 20 WB near MP 18.5, Fort Dodge .....	49
Figure 38. Seasonal FWD test results of US 59 NB near MP 95.0, Denison .....	50
Figure 39. Seasonal FWD test results of US 20 EB near MP 18.5, Merville .....	51
Figure 40. Seasonal FWD test results of US 30 WB near MP 154.85, Nevada (Nevada east) .....	52
Figure 41. Seasonal FWD test results of US 30 EB near MP 161.35, Nevada (Nevada west) .....	53
Figure 42. Seasonal FWD test results of US 218 SB near MP 214.05, Plainfield .....	54
Figure 43. DCP-CBR profiles of US 20 WB near MP 18.5, Fort Dodge .....	55
Figure 44. DCP-CBR profiles of US 59 NB near MP 95.0, Denison .....	56
Figure 45. DCP-CBR profiles of US 20 EB near MP 18.5, Merville .....	57
Figure 46. DCP-CBR profiles of US 30 WB near MP 154.85, Nevada (Nevada east) .....	58
Figure 47. DCP-CBR profiles of US 30 EB near MP 161.35, Nevada (Nevada west) .....	59
Figure 48. DCP-CBR profiles of US 218 SB near MP 214.05, Plainfield .....	60
Figure 49. US 20 WB near MP 18.5, Fort Dodge on 02/24/2011 .....	61
Figure 50. US 20 WB near MP 18.5, Fort Dodge on 08/04/2011 .....	62
Figure 51. US 20 WB near MP 18.5, Fort Dodge on 11/15/2011 .....	63
Figure 52. US 59 NB near MP 95.0, Denison on 02/24/2011 .....	64
Figure 53. US 59 NB near MP 95.0, Denison on 08/03/2011 .....	65
Figure 54. US 59 NB near MP 95.0, Denison on 11/16/2011 .....	66
Figure 55. US 20 EB near MP 18.5, Merville on 02/24/2011 .....	67
Figure 56. US 20 EB near MP 18.5, Merville on 08/03/2011 .....	68
Figure 57. US 20 EB near MP 18.5, Merville on 11/16/2011 .....	69
Figure 58. US 30 WB near MP 154.85, Nevada (Nevada east) on 03/03/2011 .....	70
Figure 59. US 30 WB near MP 154.85, Nevada (Nevada east) on 08/08/2011 .....	71
Figure 60. US 30 WB near MP 154.85, Nevada (Nevada east) on 11/17/2011 .....	72
Figure 61. US 30 EB near MP 161.35, Nevada (Nevada west) on 03/03/2011.....	73
Figure 62. US 30 EB near MP 161.35, Nevada (Nevada west) on 08/08/2011.....	74
Figure 63. US 30 EB near MP 161.35, Nevada (Nevada west) on 11/17/2011.....	75
Figure 64. US 218 SB near MP 214.05, Plainfield on 02/26/2011.....	76
Figure 65. US 218 SB near MP 214.05, Plainfield on 08/04/2011.....	77
Figure 66. US 218 SB near MP 214.05, Plainfield on 11/15/2011.....	78

## LIST OF TABLES

Table 1. FWD indices (Drumm and Meier 2003).....	13
Table 2. Summary of the project sites .....	18
Table 3. Summary of field testing dates, tests, and locations on the test section .....	19



## ACKNOWLEDGMENTS

This research was conducted under Federal Highway Administration (FHWA) DTFH61-06-H-00011 Work Plan 18 and the FHWA Pooled Fund Study TPF-5(183), involving the following state departments of transportation:

- California
- Iowa (lead state)
- Michigan
- Pennsylvania
- Wisconsin

The authors would like to express their gratitude to the National Concrete Pavement Technology (CP Tech) Center, the FHWA, the Iowa Department of Transportation (DOT), and the other pooled fund state partners for their financial support and technical assistance.

Chris Brakee, Melissa Serio, and several others with the Iowa Department of Transportation provided assistance in identifying the project, providing access to the project site, and obtaining project design information and specifications. We greatly appreciate their help.

We than Jiake Zhang, Cheng Li, Luke Johanson, and Brian Zimmerman of Iowa State University for their help with laboratory testing and Christianna White for comments and editorial assistance.



## LIST OF SYMBOLS AND ACRONYMS

CBR	California bearing ratio
CBR <sub>SB</sub>	CBR of subbase determined from DCP test
CBR <sub>SG</sub>	CBR of subgrade determined from DCP test
CBR <sub>SG-Weak</sub>	CBR of weak layer subgrade determined from DCP test
DPI	Dynamic penetration index
D <sub>0</sub>	Deflection measured under the plate
$k$	Modulus of subgrade reaction
$k_{\text{FWD-Dynamic-Corr}}$	Dynamic modulus of subgrade reaction from FWD test
$k_{\text{FWD-Static-Corr}}$	Static modulus of subgrade reaction from FWD test
M <sub>r</sub>	Resilient modulus
R <sup>2</sup>	Coefficient of determination



## EXECUTIVE SUMMARY

Quality foundation layers (i.e., the natural subgrade, subbase, and embankment) are essential to achieving excellent pavement performance. Unfortunately, many pavements in the United States still fail due to inadequate foundation layers. To address this problem, a research project, Improving the Foundation Layers for Pavements (FHWA DTFH 61-06-H-00011 WO #18; FHWA TPF-5(183)), was undertaken by Iowa State University (ISU) to identify, and provide guidance for implementing, best practices regarding foundation layer construction methods, material selection, in situ testing and evaluation, and performance-related designs and specifications. As part of the project, field studies were conducted in several in-service concrete pavements across the country that represented either premature failures or successful long-term pavements. A key aspect of each field study was to tie performance of the foundation layers to key engineering properties and pavement performance. In situ foundation layer performance data, as well as original construction data and maintenance/rehabilitation history data, were collected and geospatially and statistically analyzed to determine the effects of site-specific foundation layer construction methods, site evaluation, materials selection, design, treatments, and maintenance procedures on the performance of the foundation layers and of the related pavements. A technical report was prepared for each field study.

In this study, detailed field testing was conducted with the objective of measuring the seasonal variations in the field  $k$  values and comparing them with what was assumed in the design. This field testing was conducted by using a Kuab FWD and DCP testing on five different pavement test sections in the State of Iowa eight times over a two-year period (July 2010 to July 2012) in different seasons (winter, spring, summer, and fall). The pavement test sections varied in age from 6 to 56 years and showed varying levels of distress and ride quality (very poor to good) at the time of testing. The Iowa DOT provided pavement condition index (PCI) values for the test sections, based on testing performed in 2011. The PCI values are compared with the in situ test measurements in this report.

Testing was conducted when the foundation layers were in frozen condition (winter), thawed condition, and in equilibrium condition (summer and fall). DCP testing was conducted by drilling a hole in the pavement, and directly testing the foundation layer properties down to about 2 m below the surface. Both FWD and DCP test results were analyzed to estimate the  $k$  values and assess the differences in the estimated values. At one of the test sites, temperatures of the foundation layers were continuously monitored during the testing period. FWD testing was conducted to determine the modulus of subgrade reaction ( $k$ ) values. DCP testing was conducted to estimate California bearing ratio (CBR) values of the foundation layers. Temperature data was analyzed to determine freezing and thawing periods and frost penetrations in the foundation layers. Seasonal variations observed in the foundation mechanistic properties were compared with the assumed design values. The  $k$  values determined from FWD testing are compared with the  $M_r$  values determined from DCP testing, in relationship with the empirical models used in the design procedures to convert  $k$  to  $M_r$ .

The key findings from this study are as follows:

- On average, there was no significant difference in  $k_{\text{FWD-Static-Corr}}$  values obtained in thawed condition and summer at any of the sites. The CBR values also did not show significant differences between thawed condition and summer at most of the sites, except at the Plainfield site where  $\text{CBR}_{\text{SG-Weak}}$  increased from about 10 in thawed state to about 40 in summer. The  $k_{\text{FWD-Static-Corr}}$  values in frozen condition was about 10% to 56% higher than in summer at four of the five sites. At one test site, the values were about the same at all testing times.
- At two of the five sites, the  $k_{\text{FWD-Static-Corr}}$  values were about 1.5 to 2 times lower than the design assumed  $k$  value (41 kPa/mm) in thawed condition and in summer.
- Results indicated that the  $M_{\text{r-SG}}$  values were unrealistically high when compared with the  $k_{\text{FWD-Static-Corr}}$ .  $M_{\text{r-SG-Weak}}$  were much lower than the  $M_{\text{r-SG}}$  values. A simple linear regression fit was applied to  $M_{\text{r-SG-Weak}}$  versus  $k_{\text{FWD-Static-Corr}}$  results, which yielded a  $R^2$  of 0.45 with RMSE of 11.2 kPa/mm for  $k$  values. Compared to the linear regression fit in the data, use of the AASHTO model significantly over estimates the  $k$  values.
- It is important for designers and practitioners to recognize this uncertainty in the estimated values when using empirical relationships, and also the differences that exist between the values calculated from the different test methods. Also, it must be noted that  $k$  and  $M_{\text{r}}$  are stress-dependent parameters and most of the empirical relationships between CBR vs.  $M_{\text{r}}$  and  $M_{\text{r}}$  vs.  $k$  do not properly address this issue.
- Relationship between pavement age and PCI showed a strong linear trend with  $R^2 > 0.93$ . Similar linear regression relationship was documented by White and Vennapusa (2014) based on testing on low volume jointed PCC pavement test sites.
- The relationship between  $k_{\text{FWD-Static-Corr}}$  and PCI yielded a strong linear regression relationship with  $R^2 > 0.95$ , while the relationship between  $\text{CBR}_{\text{SG-Weak}}$  and PCI yielded a strong non-linear exponential trend with PCI with  $R^2 > 0.95$ . These trends suggest that higher foundation layer stiffness or strength provide a better ride quality and that ride quality is influenced by pavement age. Although additional testing is warranted to further explore and validate these empirical models, an advantage of having these models is that designers can use them to target a desired ride quality for a target design age by controlling foundation layer mechanistic properties.



## CHAPTER 1. INTRODUCTION

Pavements in northern hemisphere are subjected to seasonal temperature variations with freeze-thaw cycles that affect both pavement surfaces and foundation layers. Potential damages from freeze-thaw cycles include frost induced vertical heave, surface cracks, pumping of fines under traffic loading, and loss of support that reduces ride quality. Pavement foundation mechanistic characteristics such as stiffness and strength, are significantly influenced by seasonal temperature variations and therefore have to be properly characterized as it has implications to design, construction, maintenance, and serviceability (Brandl, 2008; Solanki et al., 2013; White et al., 2013).

Various thickness design procedures have been developed since the 1970s for concrete pavement design. PCA (1984) and AASHTO (1993) design procedures are currently the most popularly used methods by the highway agencies in the U.S., while there is increasing interest in implementing the newly developed mechanistic-empirical design guide (AASHTO, 2008). While the AASHTO (2008) procedure is a significant advancement over the PCA (1984) and AASHTO (1993) procedures in terms of analyzing the pavement responses, the key design parameter used to characterize foundation layer support is still the modulus of subgrade reaction ( $k$ ) value. Resilient modulus ( $M_r$ ) value is one of design parameters in AASHTO (1993) and AASHTO (2008), but the  $M_r$  value is converted to  $k$  value using empirical relationships in the design process. AASHTO (1993) provides suggested values for use in design as target  $M_r$  values for subgrade in frozen, thawed, and summer conditions. AASHTO (2008) deals with seasonal variations in a much more sophisticated manner based on local climatic modeling data and laboratory test measurements to adjust modulus values for seasonal variations.

The  $k$  value is determined using a static plate load test, which can be time consuming and expensive to setup. Therefore, various alternative testing methods have been in use by highway agencies to empirically determine the  $k$  value. Deflection tests using falling weight deflectometer (FWD) is a popular choice for determining  $k$  value based on testing performed on pavement surface layers (Puppala, 2008; AASHTO, 1993; AASHTO, 2008). Dynamic cone penetrometer (DCP) test is another test device that has been recommended in the AASHTO (2008) design guide as a method to determine California bearing ratio (CBR), which is then empirically correlated to  $k$  value.

Most highway agencies assume  $k$  values during the design phase either based on experience from historically available data or limited field testing. For rehabilitated pavement designs, agencies in the U.S. typically use FWD testing data on the existing pavements, while for new pavements, CBR or  $M_r$  testing is typically performed on samples obtained from the field.

In this study, detailed field testing was conducted with the objective of measuring the seasonal variations in the field  $k$  values and compare them with what was assumed in the design. This field testing was conducted by using a Kuab FWD and DCP testing on five pavement test sections in the State of Iowa eight times over a two year period (July 2010 to July 2012) in different seasons (winter, spring, summer, and fall). The pavement test sections varied in age from 6 to 56 years and showed varying levels of distress and ride quality (very poor to good) at

the time of testing. The Iowa DOT provided pavement condition index (PCI) values for the test sections based on testing performed in 2011. The PCI values were compared with the in situ test measurements in this report.

Testing was conducted when the foundation layers were in frozen condition (winter); thawed condition (late winter/spring); and in equilibrium conditions (summer and fall). DCP testing was conducted by drilling a hole in the pavement and directly testing the foundation layer properties down to about 2 m below the surface. Both FWD and DCP test results were analyzed to estimate  $k$  values and assess the differences in the estimated values. At one of the test sites, temperatures of the foundation layers were continuously monitored during the testing period. FWD testing was conducted to determine the modulus of subgrade reaction ( $k$ ) values. DCP testing was conducted to estimate California bearing ratio (CBR) values of the foundation layers. Temperature data was analyzed to determine freezing and thawing periods and frost penetrations in the foundation layers. Seasonal variations observed in the foundation mechanistic properties were compared with the assumed design values. The  $k$  values determined from FWD testing were compared with the  $M_r$  values determined from DCP testing in relationship with the empirical models that convert  $k$  to  $M_r$  that are used in design procedures.

This report contains six chapters. Chapter 2 provides project background information with a review of literature on topics related to seasonal variation in pavement and foundation layers. Chapter 3 presents an overview of the experimental test sections and the testing methods used in this project. Chapter 4 presents the in situ test results and data analysis. Chapter 5 presents key findings and conclusions from this study.

The findings from this report should be of significant interest to researchers, practitioners, and agencies who deal with design, construction, and maintenance aspects of PCC pavements. Results from this project provide one of several field project reports developed as part of the TPF-5(183) and FHWA DTFH 61-06-H-00011:WO18 studies.

## **CHAPTER 2. BACKGROUND**

This chapter presents brief background information on the projects, photos taken during in situ testing, and a review of literature review related to seasonal variation.

### **Seasonal Freeze-Thaw Cycles in Pavements and Foundation Layers**

When pavement structures are exposed to frost heaving and thaw weakening, the mechanical properties can be significantly affected by the seasonal changes in temperature and soil moisture conditions (Simonsen and Isacsson 1999). Simonsen and Isacsson reviewed the available literature on the effects of freezing and thaw weakening on pavement structures. The stiffness of supporting layers typically increases when frozen because soil particles in the base and subbase materials are frozen together and ice lens have formed in the subgrade materials, which result in an increase in bearing capacity. The damage caused by freezing is due to differential frost heave and thermal cracks in asphalt cement (AC) layers. According to Simonsen and Isacsson (1999), once pavements begin to thaw in the spring, bearing capacity can be drastically reduced because of increased saturation in the supporting layers. They reported that drainage in pavement systems is very important in general, but it is even more important in cold regions because increases in moisture content in foundation layers when water from thawing ice causes high pore water pressures to develop that lead to reductions in effective stress that influences shear stress and bearing capacity. Further, water that results from melting ice becomes trapped between the pavement material and the remaining frozen layers below (Simonsen and Isacsson 1999).

Simonsen and Isacsson (1999) also reported that less severe winters produce conditions for larger amounts of heave for given depths of frost because slow frost penetration rates can result in more ice lenses being formed. This slow frost penetration leads to the majority of the ice accumulating near the surface of the pavement foundation layers. Once the ice begins to melt, there is a rapid release of water that can create detrimental support conditions. On the other hand, severe winters result in deeper frost penetration, which means that the main concentrations of ice are deeper in the pavement foundation. Even though there may be more ice present, the effect of the melting ice on the pavement is less rapid and spread over a longer period of time. If drainage of the pavement system is high enough, the effects of additional water on the system will be lessened. The ability of the system to drain is related to the fines content of the materials.

According to Johnson (2012), thawing typically progresses from the pavement surface down and results in conditions where melted water can become trapped between the pavement surface and the frozen layers below. In this condition, where thawing is rapid, the drainage path is constrained in the vertical direction so transverse drainage paths must be available. When this occurs, transverse drainage can be cut off. If slower thawing takes place, the thawing front will work its way from the lower layers up and water will be allowed to drain. The thaw depth affects the amount of settlement that will take place and the rate of thawing affects the magnitude of change in pore water pressure. The amount of settlement that takes place depends on ice lens formation, soil density, pore water pressures, and soil compressibility.

Simonsen and Isacsson (1999) found that the following factors can impact the amount of thaw-weakening damage on pavement systems: road structure, frost susceptibility, subgrade conditions, temperature, precipitation, and traffic. They found that the length of recovery from thaw weakening is dependent on the frost depth, soil type, water content, and drainage conditions. It can take weeks to months to fully recover, depending on the drainage conditions. Andersland and Ladanyi (2004) suggested that load restrictions can be used to reduce pavement damage during periods of thaw weakening, but that load restrictions are most commonly used on flexible pavements because most rigid pavements were determined to be able to resist the loss of strength during thawing.

Simonsen and Isacsson (1999) described that when pavement foundation layers are deformed under traffic loads, most of the deflection rebounds once the load has been removed. The remaining deformation that does not rebound is called permanent deformation and occurs when excess water is present. Spring thawing conditions present the ideal opportunity for permanent deformation to occur. When base materials are saturated, vehicle loads are initially placed on the pore water. When the pore water is loaded it makes the base material unstable and can cause upward stress that can cause cracks in the pavement system. After this process occurs many times, it can cause holes in the pavement layer and a loss of base material; this is especially true for AC pavements. Salour and Erlingsson (2012) found that when the base course is saturated, there can be a pumping of fines in the base course which eventually leads to a weaker and less drainable material than what was initially designed.

Another type of failure can occur when the subgrade is frost susceptible and has been frozen (Simonsen and Isacsson 1999). Once, the subgrade begins to thaw and the pore water pressures increase due to the additional water, the subgrade is displaced and is unable to sustain the loads that are applied from the upper pavement layers. When the subgrade is displaced, a loss of support for the pavement layer occurs which can cause deformations in the pavement. Salour and Erlingsson (2012) found that the relative damage on AC pavements caused by traffic loading during thaw weakening is 1.5 to 3 times higher than the average annual damage.

Andersland and Ladanyi (2004) reported that determining the 0°C isotherm is an approach to analyze temperature variations in pavement focusing on freezing and thawing periods in pavement layers (Figure 1). Frozen and thawed zones versus time can be estimated from the isotherm depth. Determination of this isotherm presents the maximum frost penetrations and the periods that pavements are susceptible to break-up. This period is defined as the time when the upper pavement layers are thawed while the lower layers are still frozen. Thawed water from upper layers cannot drain into lower frozen layers due to the low permeability. In these conditions, the bearing capacity of foundations may significantly decrease, and the upper pavements become more fragile under traffic loads. Andersland and Ladanyi (2004) reported these fragile conditions are a problem that pavement engineers need to identify, which is the primary reason why spring load restriction needs to be implemented in seasonal frost regions (Ovik et al., 2000; NDDOT, 2015).

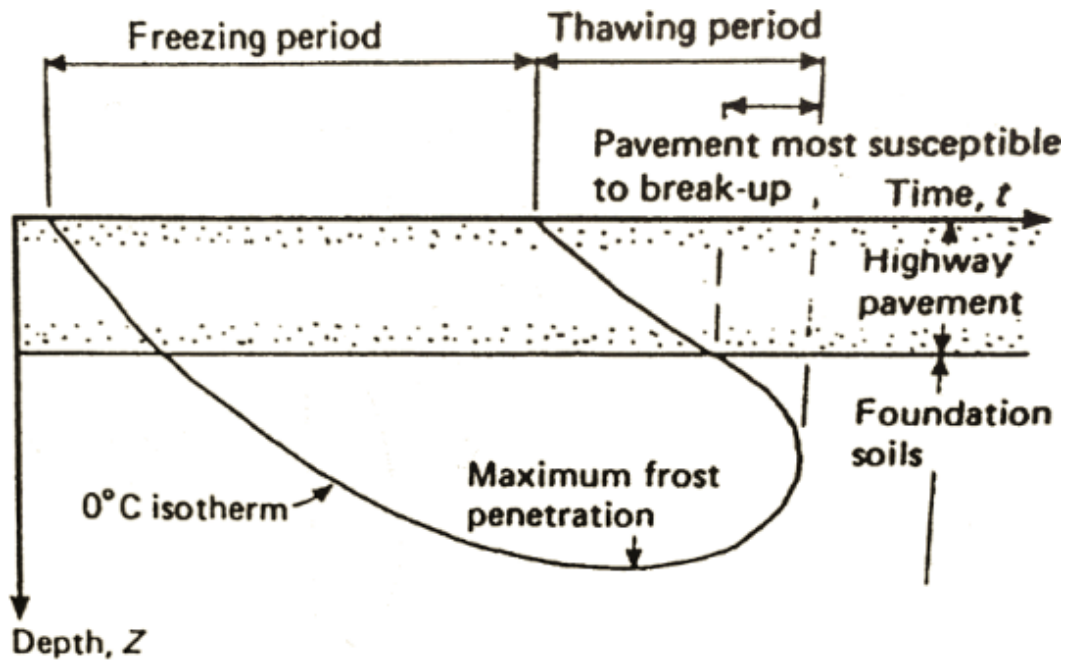


**Figure 1. Model of seasonal ground freezing and thawing periods beneath pavement (Andersland and Ladanyi 2004)**

As part of a study of soil stabilization, Hoover et al. (1962) constructed and examined a pavement test section built on US 117 in Jasper County, Iowa during October 1957. They computed  $0^{\circ}\text{C}$  isotherms and estimated frost depths using the Modified Berggren Formula and U.S. Weather Bureau information. They also estimated the number of freeze-thaw cycles that occurred during each winter cycle, as shown in Figure 2 to Figure 4.

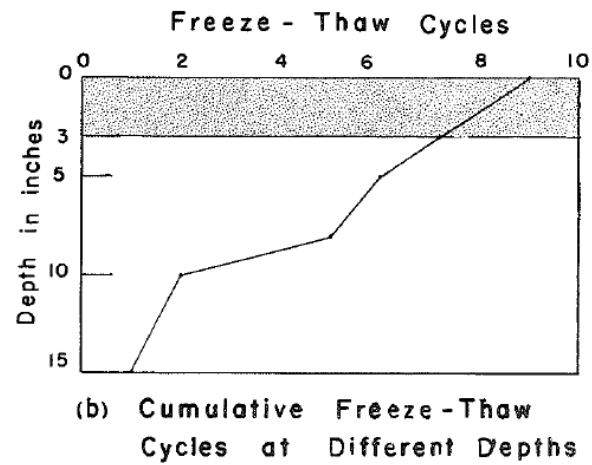
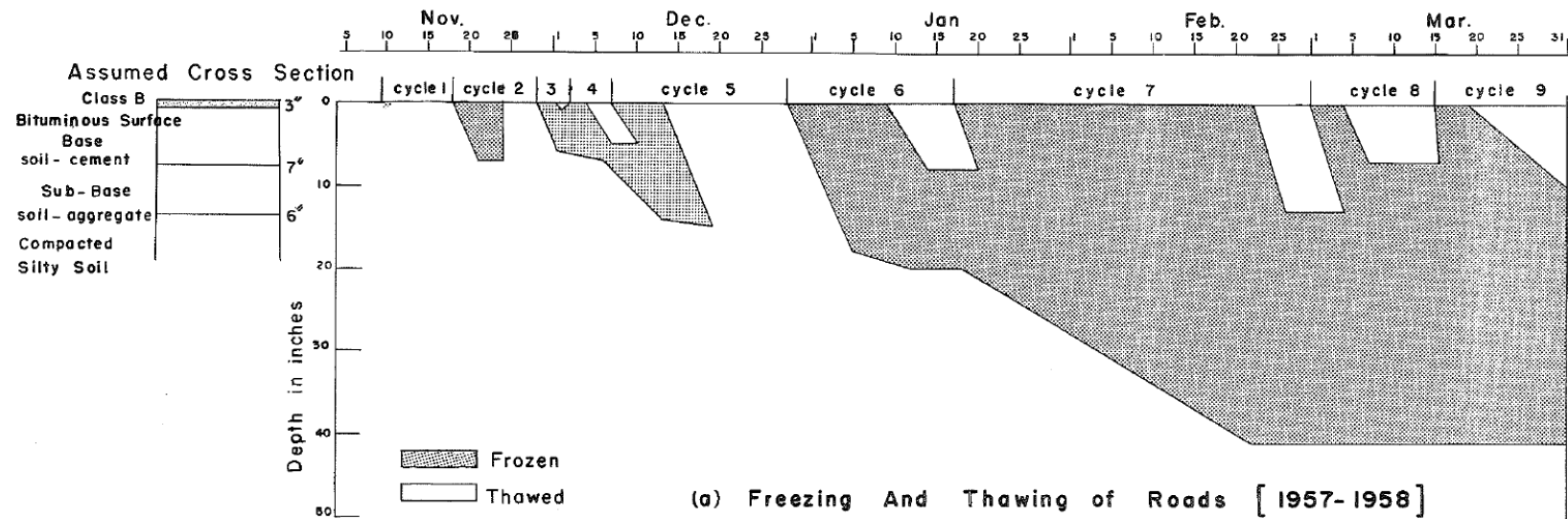
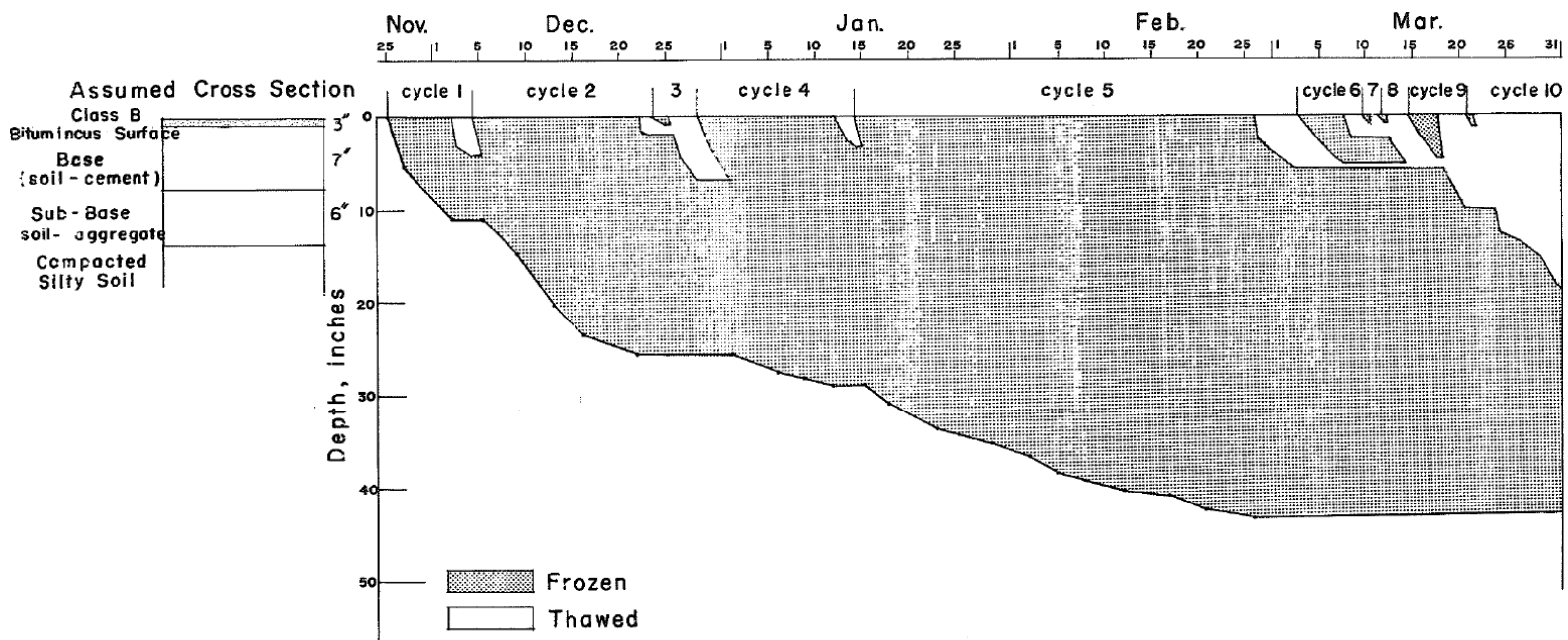


Figure 2. Winter 1957-1958: Computed frozen zones (top) and cumulative freeze-thaw cycles (bottom) (Hoover et al. 1962)





(a) Freezing And Thawing of Roads [ 1958 - 59 ]

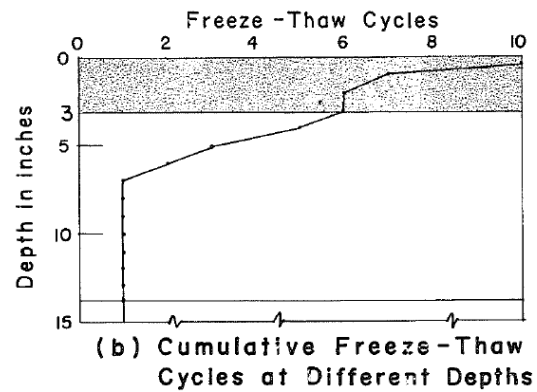


Figure 3. Winter 1958-1959: Computed frozen zones (top) and cumulative freeze-thaw cycles (bottom) (Hoover et al. 1962)

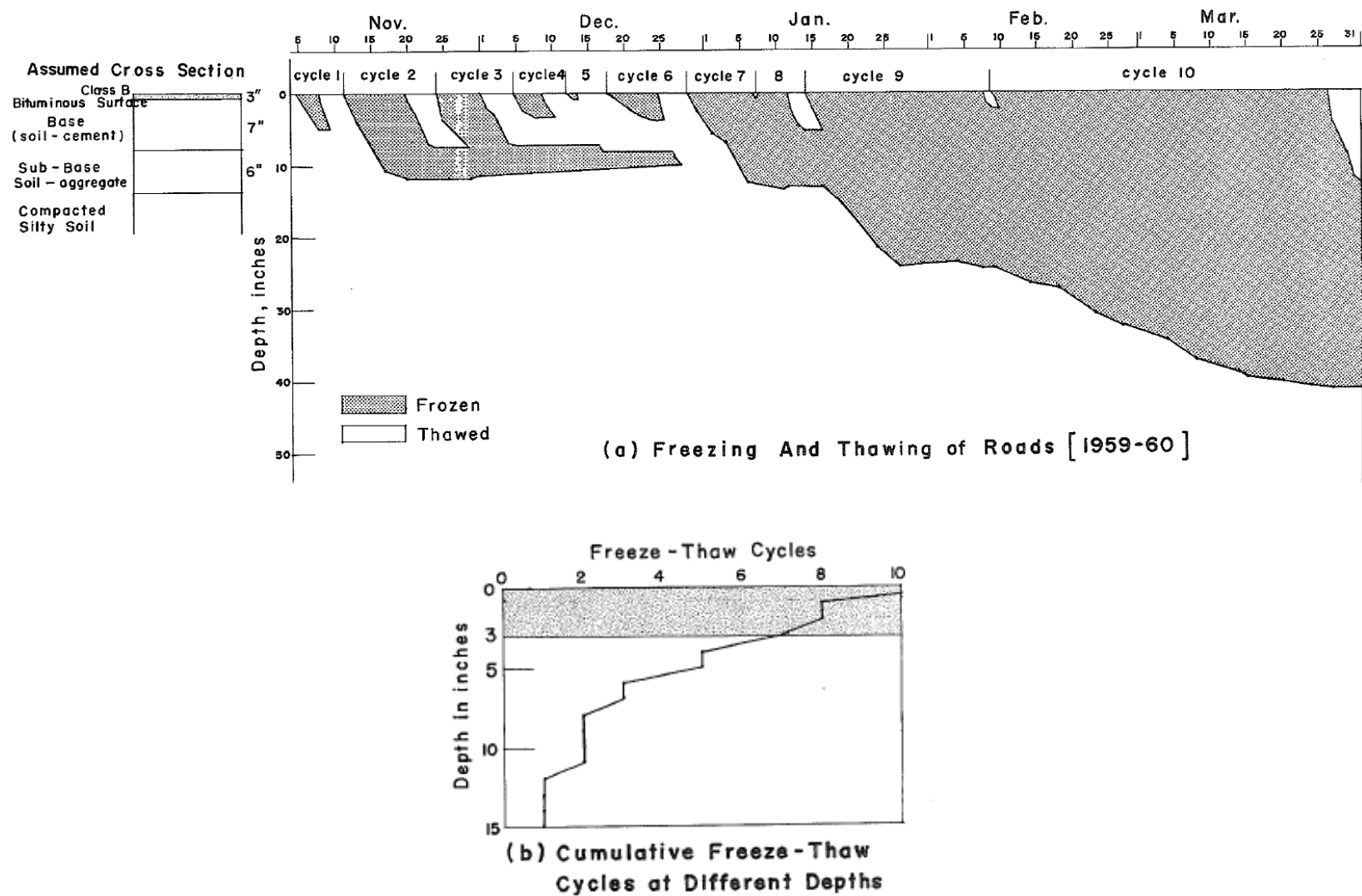


Figure 4. Winter 1959-1960: Computed frozen zones (top) and cumulative freeze-thaw cycles (bottom) (Hoover et al. 1962)

## Seasonal Variations in Pavement Foundation Mechanistic Properties

In situ testing during different seasons to determine mechanistic properties of pavement foundation layers such as strength and  $M_r$  or  $k$  is critical for thickness design because these properties of pavement foundations change in response to climatic conditions (Lary et al. 1984, Konrad and Roy, 2000). Pavement design guides take this into consideration (AASHTO, 1993; AASHTO, 2008). For example, AASHTO (1993) suggests adjusting the design  $M_r$  of roadbed soil based on the durations of periods of freezing and thawing and in summer. AASHTO (1993) provides suggested values for use in design when subgrade is in frozen, thawed, and summer conditions. AASHTO (2008) deals with seasonal variations in a more sophisticated manner that accounts for local climatic modeling data and laboratory test measurements to adjust design modulus values for seasonal variations.

The next section is a summary of the literature about field investigations into frost heave, followed by a review of the literature about thaw weakening.

### *Frost Heave*

In a study at MnRoad (Lukanen et al. 2006), frost pins were placed in sections of AC and Portland cement concrete (PCC). The AC sections had sand, clay, and granular base as foundation materials. The PCC sections had a granular base with either sand or clay underneath. The frost pins were placed at 50 ft intervals in the five 500-ft test sections and observed over a four-year period. The results revealed uneven heave across each of the sections. This differential heave affects pavement ride and performance. Differential heave can greatly increase pavement roughness and occurs when material types or properties change (e.g., a change from cut to fill or an area with increased moisture content) (Joint Departments of the Army and Air Force 1985).

Many states require a 3–5 ft subcut into the subgrade, which consists of removing the subgrade material and recompacting it in place, a process that helps create a uniform subgrade that will reduce differential heave. The test sections at MnROAD were undercut 5 ft but still showed signs of differential heave. The sections with clay subgrade in the pavement structure showed the highest amount of frost heave. Also the AC on clay sections showed an increase in the International Roughness Index (IRI) as the subgrade heaved. The AC on sand sections showed smaller increases in IRI because the subgrade had small amounts of heave. Although the PCC section with a clay subgrade heaved significantly, the PCC sections showed no increases in IRI. Lukanen et al. (2006) reported that ride quality is minimally related to differential frost heave in the subgrade and many other factors can affect the IRI in addition to frost heave. They concluded that current empirical design and mechanistic empirical design processes do not account for differential frost-heave movements.

### *Thaw Weakening*

Increased moisture content in supporting layers during thawing weakens pavement structures (Janoo and Berg 1996). This additional water in pavement structures reduces the bearing

capacity of the pavement system because reduced strength of the supporting layers. The strength of AC pavements is largely dependent on the temperature, this results in large variations in strength during the high temperature swings that occur during freezing and thawing periods. PCC can also be negatively affected during thawing periods because of curling effects that are caused by high temperature differentials in the pavement layer. The curling can occur at the edges and corners of the pavement which will affect the load transfer efficiency. Janoo and Berg (1996) conducted a study of the effects of thaw weakening on PCC for airfields. They conducted falling weight deflectometer (FWD) tests and measured temperatures in the pavement structure. Frost depths were determined based on where the temperature was 0°C. An example of their frost depth versus time can be seen in Figure 5.

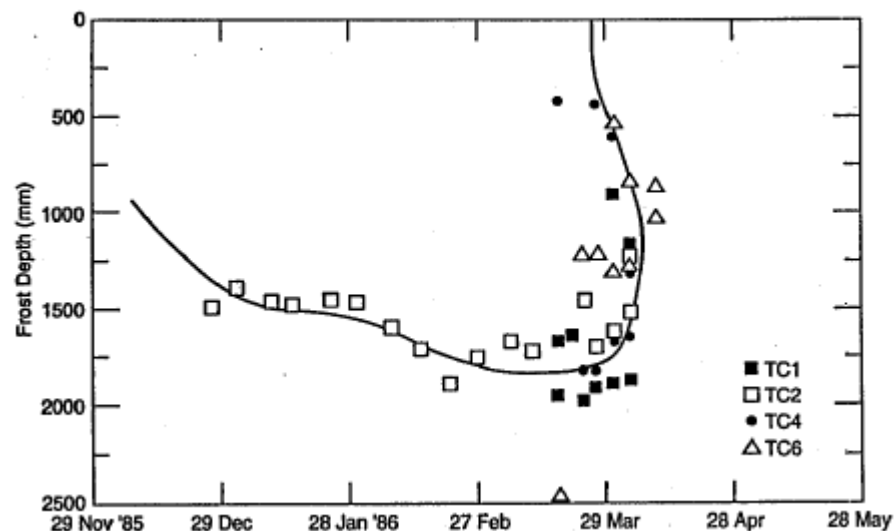


**Figure 5. Frost penetration plot (Janoo and Berg 1996)**

Janoo and Berg (1996) used the FWD deflection basin area index parameter to analyze the effects of thaw weakening. An example of the data can be seen in Figure 6. The higher the basin area measurement is, the lower the strength of the pavement structure. They measured joint load transfer efficiency (LTE), which is a measure of how well the load is distributed from one PCC slab to the next. They found that the LTE typically decreased as the temperature increased as the beginning of the spring thaw. However, as thawing progressed, the LTE began to increase (Figure 7).

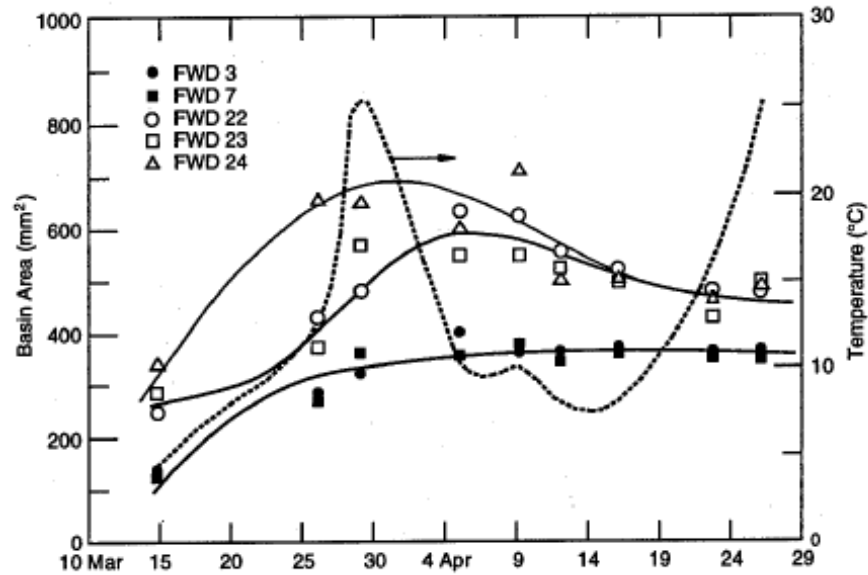


Figure 6. Change in basin area during spring thaw (Janoo and Berg 1996)

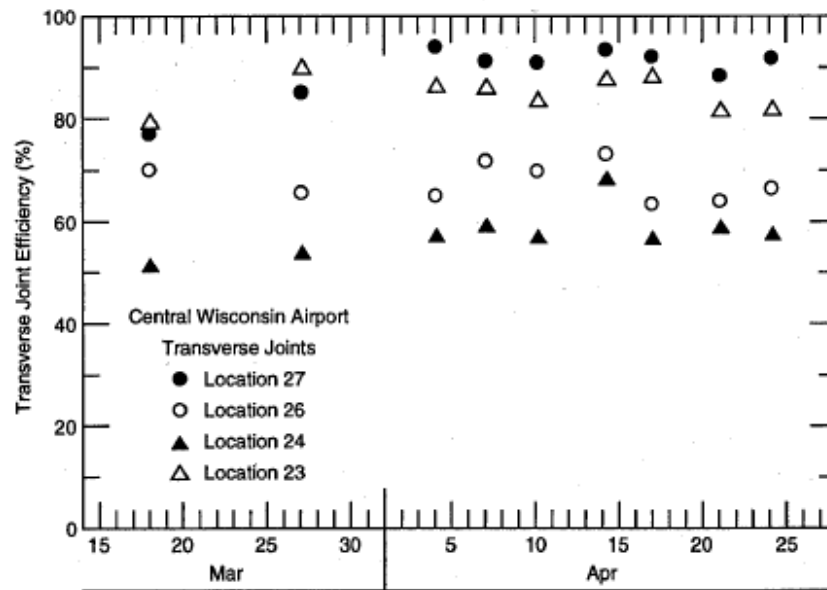


Figure 7. Joint transfer efficiency during spring thaw (Janoo and Berg 1996)

Drumm and Meier (2003) compiled seasonal test data from sites across North America. The research was conducted as a part of the Long Term Pavement Performance (LTPP) Seasonal Monitoring Program (SMP). They collected data from temperature sensors, moisture sensors, and FWD tests. They discussed that the temperature in PCC does not affect the performance as much as the gradient in the PCC slab. Curling of the slabs can result of the temperature gradient. Upward curling will occur when the temperature is cooler on the top compared to the bottom (i.e., at night) and downward curling can occur when the temperature on the top is warmer than

the bottom (i.e., during day). When the temperature in the slab is colder, the joints open which can result in reduced load transfer efficiencies. Reductions in load transfer efficiencies can also be caused by curling. FWD testing can be performed at the edge of slabs to observe daily and seasonal changes in load transfer efficiency due to curling and opening of joints. FWD deflections, from increasing loads, from the slab edges and the center of slab can be compared. If the deflections have a near linear relationship between the drop height and response, it is an indication that the slab is in good contact with the underlying layers. Any deviations from linear can indicate curling.

Drumm and Meier (2003) mentioned that it is a typical misunderstanding that granular base material do not undergo thaw weakening. This is a result of a strong base material requiring a significant amount of fines, which as discussed can decrease the permeability and increase the frost-heave potential. They found, from several sources, that there is no relationship between amount of rainfall and subgrade moisture content variation. Joint faulting in PCC, can be a result of pumping (i.e., loss of material), frost heave, or expansive subgrade soils.

Drumm and Meier stated that, “even under the best of circumstances, FWD backcalculation is as much an art as it is a science” (2003, p. 4–5). Spring thaw and recovery moduli were difficult to backcalculate because the pavement structure was not adequately modeled by the elastic layer theory that was used. Because it is difficult for theory to represent a soft saturated layer trapped between a much stiffer base material and the frost subgrade that lies below they recommended that advanced modeling would be required to represent this situation. The backcalculated moduli during frozen periods are typically too high and inconsistent. They found that it was difficult to determine when slab curling was or was not affecting the results, and recommended that deflection basins be used rather than backcalculated moduli to determine the effects of frost action on the pavement system.

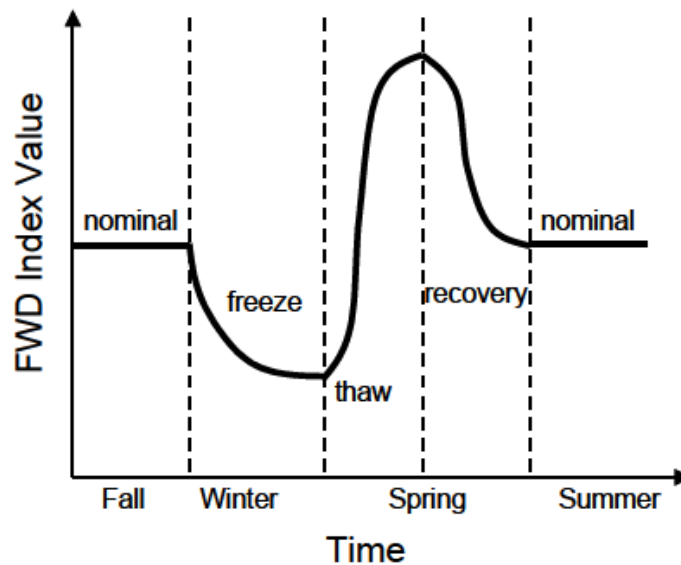
Drumm and Meier (2003) used the following indices at Mn/ROAD to assess spring thaw conditions: SCI, BDI, and  $D_0$ . The FWD indices are defined in Table 1. These indices are expected to decrease during frozen periods (Figure 8). A stress level of 550 kPa was used in the study because it corresponds to a stress level that is typically used in pavement design. With the data available, they were not able to detect a significant thaw-weakening period. They hypothesized that it was a result of one or a combination of the following factors: thaw weakening occurred between their site visits, the subgrade soils were not frost susceptible, or the pavements were designed to minimize the effects of thaw weakening. The LTPP SMP sites were only visited once a month. Drumm and Meier analyzed FWD results on AC pavements from the U.S. Army Frost Effects Research Facility and other locations that were collected on a daily basis during thawing and reported that the effects of thawing could be seen from SCI and SDI indices.



**Table 1. FWD indices (Drumm and Meier 2003)**

Parameter	Formula
AREA	$6 * [(D_0/D_0) + (2*D_{305}/D_0) + (2*D_{610}/D_0) + (D_{914}/D_0)]$
Deflection at load plate ( $D_0$ )	$D_0$
Deflection at 1524 mm ( $D_{1524}$ )	$D_{1524}$
Base curvature index (BCI)	$D_{610} - D_{914}$
Surface curvature index (SCI)	$D_0 - D_{305}$
Basin damage index (BDI)	$D_{305} - D_{610}$
Partial area (PA), $m^2$	$[(D_{457}+D_{610})/2*0.153] + [(D_{610}+D_{914})/2*0.304] + [(D_{914}+D_{1524})/2*0.610]$
Subgrade damage index (SDI)	$D_{610} - D_{1524}$
Subsurface index (SI)	$D_{305} - D_{1524}$

$D_x$  is the surface deflection measured x mm from the loading plate.

**Figure 8. Expected seasonal variation of FWD indices (Drumm and Meier 2003)**

Jong et al. (1998) performed a study to develop a method for determining when load restrictions should be implemented. The data collected measured air and subsurface temperatures, subsurface water contents, water phase changes, and pavement moduli. Thermocouples and thermistors were used to measure temperature, time domain reflectometry probes were used to determine water contents and phase changes, and FWD tests were used to determine the pavement moduli. Flexible pavements (i.e., AC pavements) were tested over an 18 month period on three secondary highways. They found that the thermocouples, thermistors, and time domain

reflectometry probes all resulted in approximately the same frost depth profiles (Figure 9). They presented the structural capacity of the pavement in the form of FWD deflection basins and backcalculated FWD moduli. An example of the FWD deflection basin can be seen in Figure 10. The basins show that the deflection is very low during winter and very high during spring, with the deflections for the summer period falling in between.

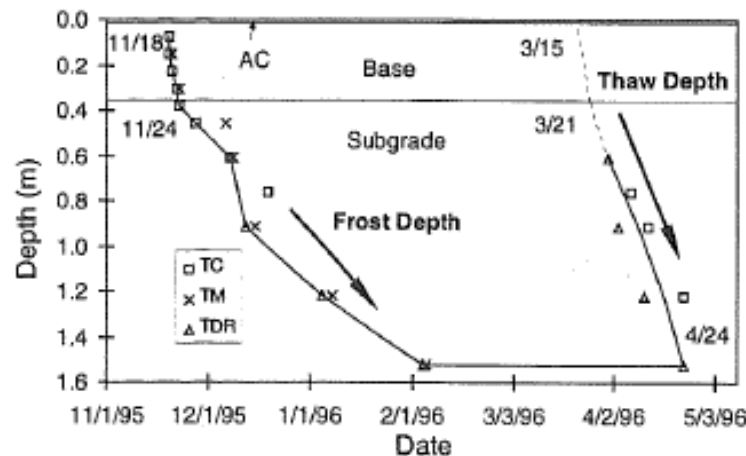


**Figure 9. Frost depth measured with thermocouples, thermistors, and time domain reflectometry probes (Jong et al. 1998)**

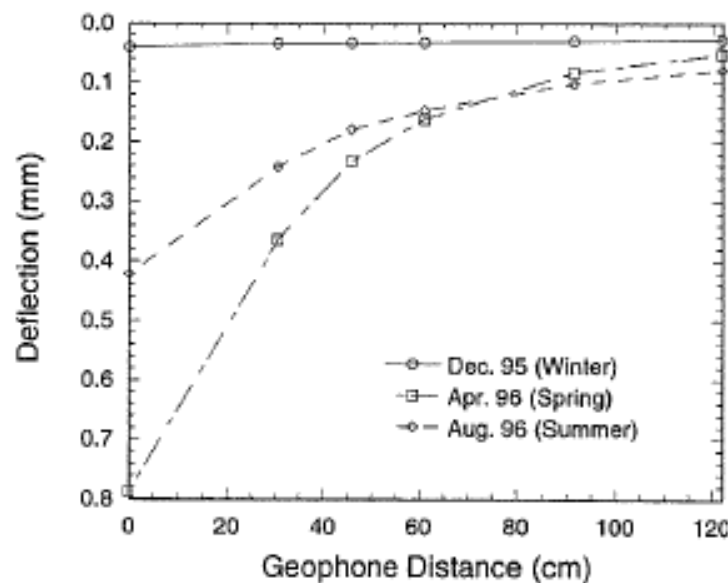


**Figure 10. Changes in seasonal FWD deflection basins (Jong et al. 1998)**

Jong et al. (1998) performed FWD tests at approximately 15 m intervals and found that overall; the modulus did not vary significantly for the intervals tested, so it was assumed that one interval could be used to represent the test section. They found that the moduli of the base and subgrade continued to weaken, after thawing began, until both layers were completely thawed (Figure 11).

The thaw weakening stage lasted approximately one month and continued to recover for an additional four months. Figure 11 also shows that the subgrade has a higher modulus than the base for a brief period during thawing.

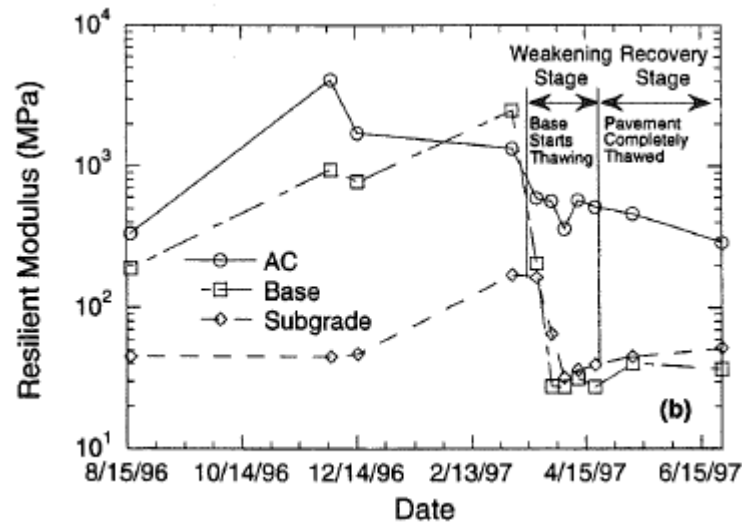


**Figure 11. Changes in seasonal resilient modulus (Jong et al. 1998)**

Newcomb and Birgisson (1999) presented a profile of typical deflection response over a year that indicates (Figure 12). The deflection response from an applied load is reduced during periods of freezing and then drastically increases during the following thaw period. They found from other studies that the critical period during thawing is when water is trapped in the base layer between the pavement and the frozen subgrade.

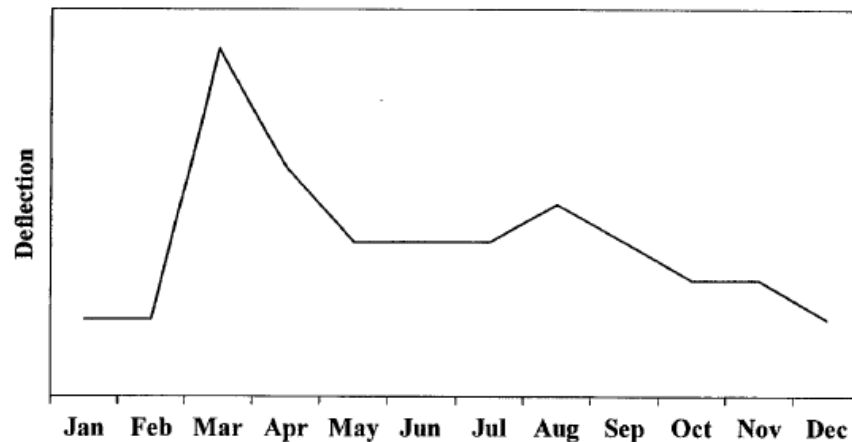


**Figure 12. Typical pavement deflection response due to seasonal changes (Newcomb and Birgisson 1999)**

The effect on the resilient modulus can be seen in (Figure 13). The result of water being trapped in the base course is that the modulus of the subgrade is actually higher than that of the base course for a short time, which supports Jong et al. (1998).

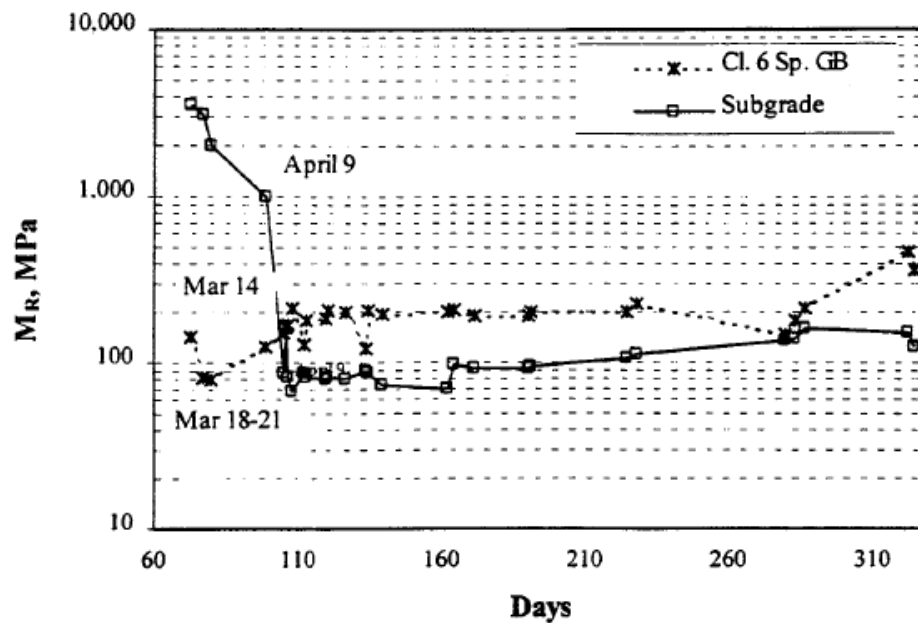


**Figure 13. Seasonal changes in the resilient moduli of base and subgrade layers (Newcomb and Birgisson 1999)**

As a part of the ROADDEX II Project in Northern Europe, the effect of thaw weakening was studied on low volume gravel roads (Saarenketo and Saara 2005). They used DCP test results to determine the changes in stiffness and thickness of pavement layers and to determine the depths to layer interfaces and the location of the frost line. They backcalculated a modulus, based on the shear strength, from the DCP data. Figure 14 shows the DCP moduli being used to track the thawing process. They concluded that the DCP test is very useful for monitoring frost depth and stiffness of the road structures, that it has problems penetrating stiff base courses so it is not suitable for observing well-built roads.

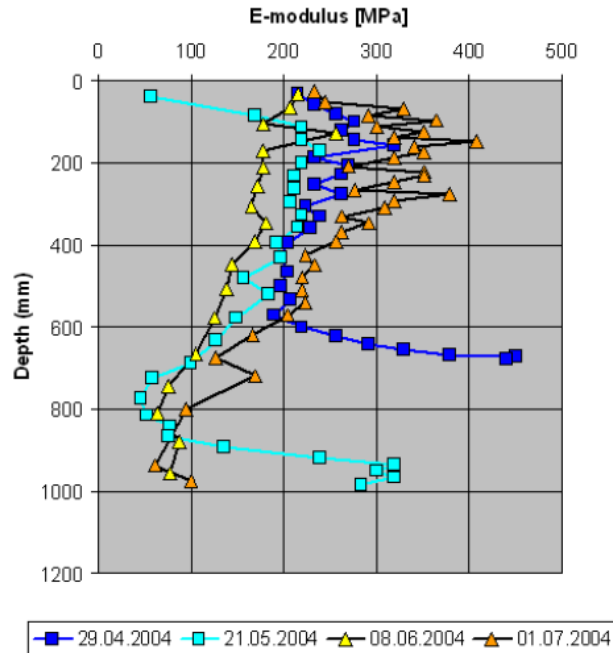


**Figure 14. Tracking thawing process by using DCP backcalculated moduli (Saarenketo and Saara 2005)**

Baladi et al. (2009) reported seasonal changes in pavement subgrade  $M_r$  values. More than 500 groups of FWD test results, including those conducted in that study and those collected within the previous 20 years, were used to determine layer moduli. The backcalculated  $k$  values from FWD deflections per empirical AREA method were converted to  $M_r$  based on AASHTO (1993). The converted  $M_r$  values were also correlated with previous data to consider limitations in applying the AASHTO (1993) conversion process to determine effects on subbase and base layers. FWD tests were conducted on two PCC and one ACC pavement test sections in Michigan during fall and spring. The results indicated that during thawing, the subgrade  $M_r$  under the PCC pavements were 30–50% less than in the fall, but subgrade  $M_r$  under the ACC pavement exhibited similar values in both seasons.

Becker et al. (2014) investigated the freeze-thaw performance of stabilized pavement foundations in Iowa from October 2012 to April 2013 by comparing the CBR and elastic modulus in the fall and after the spring thaw. Although several stabilization methods had been used, in comparison with the fall CBR values, the spring CBR of both granular subbase ( $CBR_{SB}$ ) and subgrade ( $CBR_{SG}$ ) decreased. Becker et al. (2014) reported that the thawed  $CBR_{SG}$  was as low as 10% of the values measured during summer/fall. Results of elastic modulus testing indicated the thawed stiffness of the composite foundation layers decreased by 20–90% compared to values observed in summer/fall.

## CHAPTER 3. EXPERIMENTAL TESTING

This chapter summarizes the in situ pavement test sections, the testing methods used in this research, and the data analysis procedures.

### Test Sections

Information about the test sections and the pavement condition index (PCI) values reported by Iowa DOT (2014) during the time of testing (2011) are summarized in Table 2. Pictures from each test section are shown in Figure 16 to Figure 21.

The project sites varied in pavement age from 6 years to 56 years at the time of testing, and the ride quality varied between very poor to good conditions. Four of the five sections consisted of jointed full depth portland cement concrete (PCC) pavement, while one section consisted of an asphalt overlay over jointed PCC. All sections were underlain by a nominal 254 mm thick granular subbase. Based on the information provided on Iowa DOT (2014), the granular subbase consisted of crushed limestone at four sites.

**Table 2. Summary of the project sites**

Test section ID	Project site	Year pavement built	Pavement thickness	Granular subbase material and thickness	PCI (Rating)
TS1	US 20 WB, MP 18.5, Fort Dodge	PCC 2005	254 mm	CLS, 254 mm	87 (Good)
TS2	US 59, NB, MP 95.0, Denison	ACC 1987	114 mm	CLS, 254 mm	55 (Fair)
		PCC 1971	203 mm		
TS3	US 20, EB, MP 18.5, Moville	PCC 1958	254 mm	Information on material type not available; 254 mm (interpreted from field testing)	18 (Very Poor to Serious)
TS4	US 30, WB, MP 154.85, Nevada (Nevada east)	PCC 1992	254 mm	CLS, 254 mm	82 (Satisfactory)
	US 30, EB, MP 161.35, Nevada (Nevada west)	PCC 1998			91 (Good)
TS5	US 218, SB MP 214.05, Plainfield*	PCC 2002	241 mm	CLS, 254 mm	94 (Good)

Note: MP = milepost; CLS = crushed limestone; \* pavement temperature was monitored at the site.

**Table 3. Summary of field testing dates, tests, and locations on the test section**

<b>Project site</b>	<b>Testing Dates</b>	<b>Number of Test Locations</b>
US 20 WB, MP 18.5, Fort Dodge	FWD: 5/11/2010; 7/28/2010; 11/18/2010; 2/24/2011; 3/16/2011; 8/4/2011; 11/15/2011; 3/22/2012 DCP: 11/18/2010; 3/16/2011; 8/4/2011; 11/15/2011; 3/22/2012	FWD at mid-panel: 7 FWD at joint: 7 DCP: 1
US 59 NB, MP 95.0, Denison	FWD: 5/11/2010; 7/16/2010; 11/11/2010; 2/26/2011; 3/16/2011; 8/3/2011; 11/16/2011; 4/6/2012 DCP: 11/11/2010; 2/24/2011; 3/16/2011; 8/3/2011; 11/16/2011; 4/5/2012	FWD at mid-panel: 7 FWD at joint: 7 DCP: 1
US 20 EB, MP 18.5, Merville	FWD: 5/11/2010; 7/16/2010; 11/11/2010; 2/24/2011; 3/16/2011; 8/3/2011; 11/16/2011; 4/5/2012 DCP: 11/11/2010; 3/16/2011; 8/3/2011; 11/16/2011; 4/5/2012	FWD at mid-panel: 8 FWD at joint: 8 DCP: 1
US 30 WB, MP 154.85, Nevada (Nevada east)	FWD: 5/14/2010; 7/28/2010; 11/18/2010; 3/3/2011; 3/15/2011; 8/8/2011; 11/17/2011; 3/23/2012 DCP: 11/18/2010; 3/3/2011; 3/15/2011; 8/8/2011; 11/17/2011; 3/23/2012	FWD at mid-panel: 6 FWD at joint: 6 DCP: 1
US 30 EB, MP 161.35, Nevada (Nevada west)	FWD: 5/14/2010; 7/28/2010; 11/18/2010; 3/3/2011; 3/15/2011; 8/8/2011; 11/17/2011; 6/6/2012 DCP: 11/18/2010; 3/3/2011; 3/15/2011; 8/8/2011; 11/17/2011; 6/6/2012	FWD at mid-panel: 5 FWD at joint: 5 DCP: 1
US 218 SB MP 214.05, Plainfield	FWD: 5/13/2010; 7/28/2010; 11/18/2010; 2/26/2011; 3/3/2011; 3/15/2011; 3/24/2011; 8/4/2011; 11/15/2011; 3/22/2012 DCP: 11/18/2010; 2/26/2011; 3/3/2011; 3/15/2011; 3/23/2011; 8/4/2011; 11/15/2011; 3/23/2012	FWD at mid-panel: 7 FWD at joint: 7 DCP: 1

Temperature sensor data was available at Merville, Denison, and Plainfield test sites through Iowa State Environmental Mesonet (2012). The temperature probes began at approximately 25 mm below the pavement surface and continued to a depth of about 1.8m below surface. The frost depth was determined at 2 P.M. for each day during the freezing and thawing periods. The frost depth was chosen when the temperature was at or below 0°C during freezing and at or above 0°C during thawing. Several temperature sensors failed at the Merville and Denison site in 2010, so the data from those sites were not sufficient for analysis. Only temperature data from Plainfield site data is used in the analysis presented in this report.

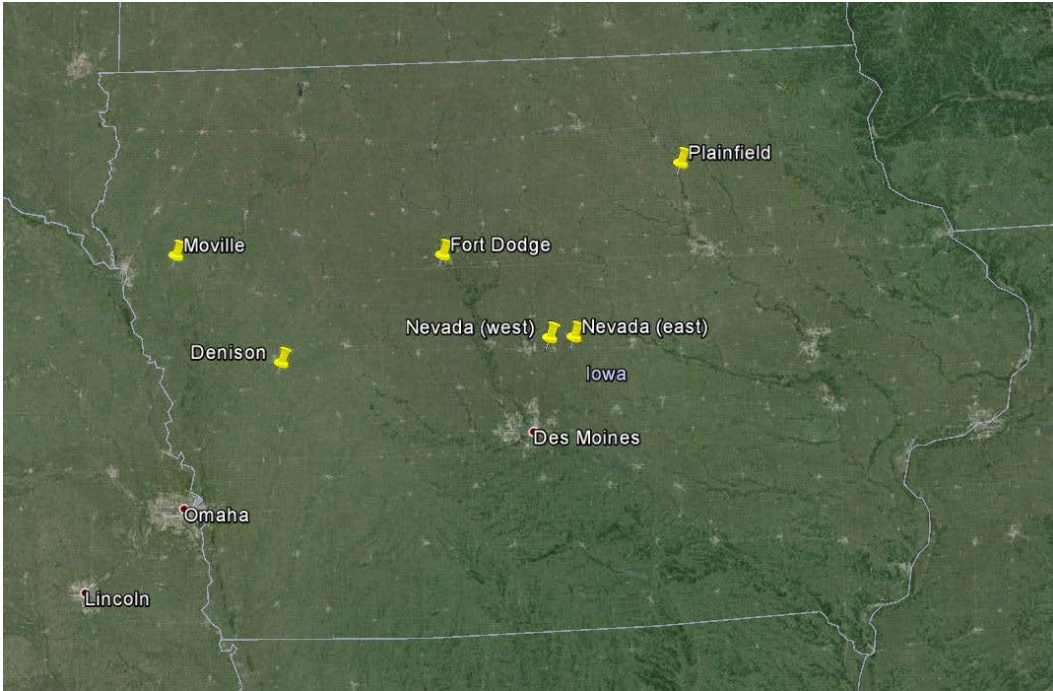


**Figure 15. Map showing the in situ test sites**



**Figure 16. TS1: US 20 WB near Fort Dodge**





**Figure 17. TS2: US 59 NB near Denison**



**Figure 18. TS3: US 20 EB near Menville**



**Figure 19. TS4: US 30 WB near Nevada (Nevada east)**



**Figure 20. TS4: US 30 EB near Nevada (Nevada west)**





**Figure 21. TS5: US 218 SB near Plainfield**

### **Kuab Falling Weight Deflectometer**

Falling weight deflectometer (FWD) tests were conducted using a Kuab FWD setup with a 300 mm (11.81 in) diameter loading plate by applying one seating drop and three loading drops. The applied loads varied from about 27 kN (6,000 lb) to 54 kN (12,000 lb) in the three loading drops. The actual applied loads were recorded using a load cell, and deflections were recorded using seismometers mounted on the device, per ASTM D4694-09 *Standard Test Method for Deflections with a Falling-Weight-Type Impulse Load Device*. The FWD plate and deflection sensor setup and a typical deflection basin are shown in Figure 22. To compare deflection values from different test locations at the same applied contact stress, the values at each test location were normalized to a 40 kN (9,000 lb) applied force.

FWD tests were conducted at the center of the PCC slab panels and at the joints. Tests conducted at the joints were used to determine joint load transfer efficiency (LTE) and voids beneath the pavement based on “zero” load intercept values. Tests conducted at the center of the slab panels were used to determine modulus of subgrade reaction ( $k$ ) values and the intercept values. The procedure used to calculate these parameters are described below.

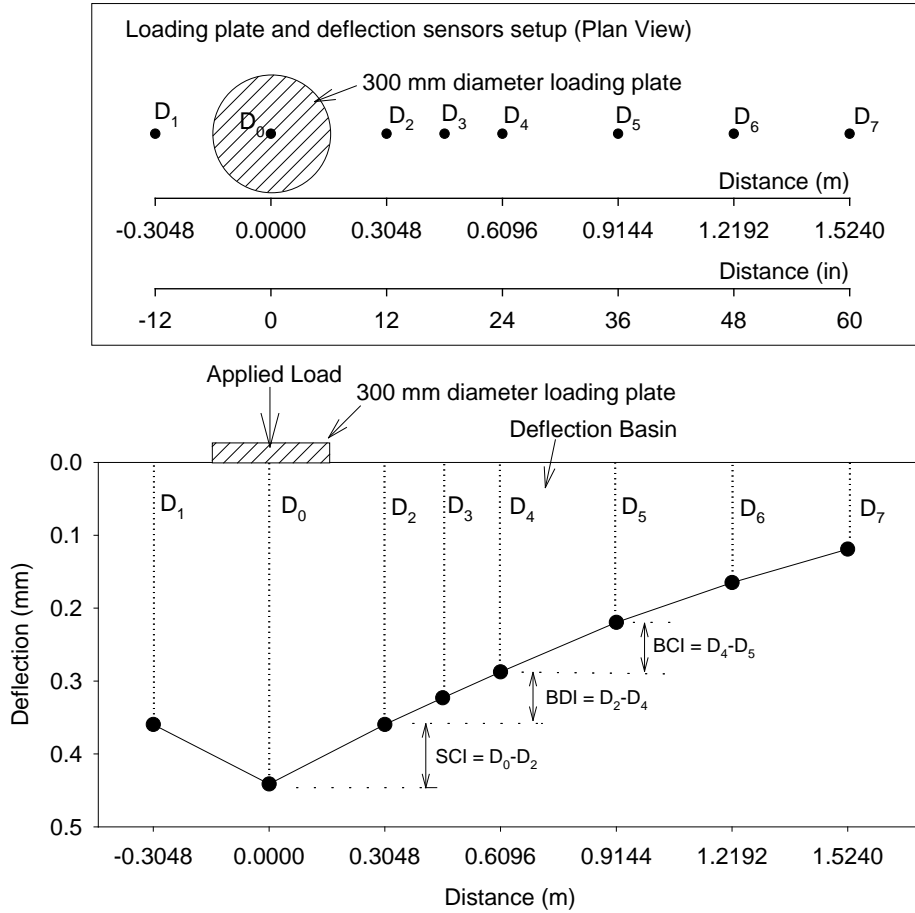


**Figure 22. FWD deflection sensor setup used for this study and an example deflection basin**

LTE was determined by obtaining deflections under the plate on the loaded slab ( $D_0$ ) and deflections of the unloaded slab ( $D_1$ ) using a sensor positioned about 305 mm (12 in.) away from the center of the plate (Figure 22). The LTE was calculated using Equation 1.

$$LTE(\%) = \frac{D_1}{D_0} \times 100 \quad (1)$$

Voids underneath pavements can be detected by plotting the applied load measurements on the X-axis and the corresponding deflection measurements on the y-axis and plotting a best fit linear regression line, as illustrated in Figure 23, to determine the “zero” load intercept (I) values. AASHTO (1993) suggests  $I = 0.05$  mm (2 mils) as a critical value for void detection. According to Quintus and Simpson (2002), if  $I = -0.01$  and  $+0.01$  mm, then the response would be considered elastic. If  $I > 0.01$  then the response would be considered deflection hardening, and if  $I < -0.01$  then the response would be considered deflection softening.

Pavement layer temperatures at different depths were obtained during FWD testing, in accordance with the guidelines from Schmalzer (2006). The temperature measurements were

used to determine equivalent linear temperature gradients ( $T_L$ ) following the temperature-moment concept suggested by Janssen and Snyder (2000). According to Vandenbossche (2005), I-values are sensitive to temperature induced curling and warping affects. Large positive temperature gradients (i.e., when the surface is warmer than the bottom) that cause the panel corners to curl down result in false negative I-values. Conversely, large negative gradients (i.e., when the surface is cooler than the bottom) that cause the panel corners to curl upward result in false positive I-values. Interpretation of I-values therefore should consider the temperature gradient. Concerning LTE measurements for doweled joints, the temperature gradient is reportedly not a critical factor (Vandenbossche 2005).

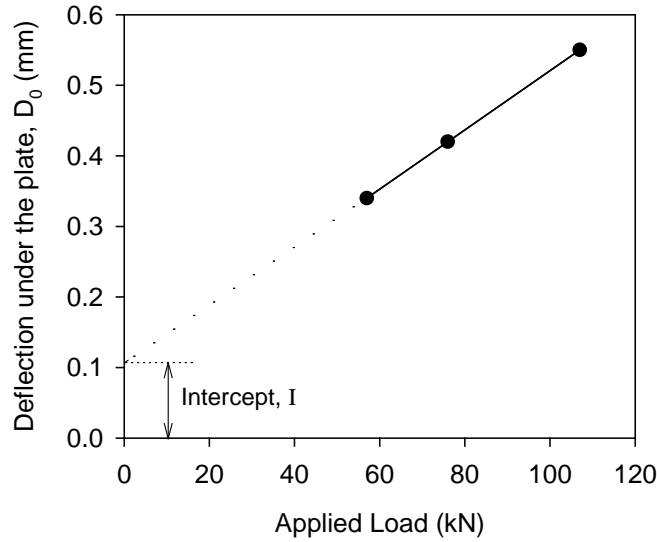


**Figure 23. Void detection using load-deflection data from FWD test**

The  $k$  values were determined using the AREA<sub>4</sub> method described in AASHTO (1993). Since the  $k$  value determined from FWD test represents a dynamic value, it is referred to here as  $k_{\text{FWD-Dynamic}}$ . Deflections obtained from four sensors ( $D_0$ ,  $D_2$ ,  $D_4$ , and  $D_5$  shown in Figure 22) were used in the AREA<sub>4</sub> calculation. The AREA method was first proposed by Hoffman and Thompson (1981) for flexible pavements and has since been applied extensively for concrete pavements (Darter et al. 1995). AREA<sub>4</sub> is calculated using Equation 2 and has dimensions of length (in inches), as it is normalized with deflections under the center of the plate ( $D_0$ ):

$$AREA_4 = 6 + 12 \times \left( \frac{D_2}{D_0} \right) + 12 \times \left( \frac{D_4}{D_0} \right) + 6 \times \left( \frac{D_5}{D_0} \right) \quad (2)$$

where  $D_0$  = deflections measured directly under the plate (in.);  $D_2$  = deflections measured at 305 mm (12 in.) away from the plate center (in.);  $D_4$  = deflections measured at 610 mm (24 in.) away from the plate center (in.); and  $D_5$  = deflections measured at 914 mm (36 in.) away from the plate center (in.). The AREA<sub>4</sub> method can also be calculated using different sensor

configurations and setups, (i.e., using deflection data from 3, 5, or 7 sensors), and those methods are described in detail in the literature (Substad et al. 2006, Smith et al. 2007)

In early research conducted using the AREA method, the ILLI-SLAB finite element program was used to compute a matrix of maximum deflections at the plate center and the AREA values by varying the subgrade  $k$ , the modulus of the PCC layer, and the thickness of the slab (ERES Consultants, Inc. 1982). Measurements obtained from FWD tests were then compared with the ILLI-SLAB program results to determine the  $k$  values through back calculation. Barenberg and Petros (1991) and Ioannides (1990) proposed a forward solution procedure based on Westergaard's solution for loading on an infinite plate to replace the back calculation procedure. This forward solution presented a unique relationship between AREA value (for a given load and sensor arrangement) and the dense liquid radius of relative stiffness ( $L$ ) in which subgrade is characterized by the  $k$  value. The radius of relative stiffness ( $L$ ) is estimated using Equation 3:

$$L = \left[ \frac{\ln \left( \frac{x_1 - AREA_4}{x_2} \right)}{x_3} \right]^{x_4} \quad (3)$$

where  $x_1 = 36$ ,  $x_2 = 1812.279$ ,  $x_3 = -2.559$ ,  $x_4 = 4.387$ . It must be noted that the  $x_1$  to  $x_4$  values vary with the sensor arrangement and these values are only valid for the AREA<sub>4</sub> sensor setup. Once, the  $L$  value is known, the  $k_{FWD-Dynamic}$  value can be estimated using Equation 4:

$$k_{FWD-Dynamic} (pci) = \frac{PD_0^*}{D_0 L^2} \quad (4)$$

where  $P$  = applied load (lbs),  $D_0$  = deflection measured at plate center (inches), and  $D_0^*$  = non-dimensional deflection coefficient calculated using Equation 5:

$$D_0^* = a \cdot e^{-be^{-cL}} \quad (5)$$

where  $a = 0.12450$ ,  $b = 0.14707$ ,  $c = 0.07565$ . It must be noted that these equations and coefficients are valid for an FWD setup with an 11.81 in. diameter plate.

The advantages of the AREA<sub>4</sub> method are the ease of use without back calculations and the use of multiple sensor data. The disadvantages are that the process assumes that the slab and the subgrade are horizontally infinite. This assumption leads to underestimating the  $k$  values of jointed pavements. Croveti (1993) developed the following slab size corrections for a square slab that is based on finite element analysis conducted using the ILLI-SLAB program and is for use in the  $k_{FWD-Dynamic}$ :

$$Adjusted D_0 = D_0 \left( 1 - 1.15085e^{-0.71878 \left( \frac{L'}{L} \right)^{0.80151}} \right) \quad (6)$$

$$Adjusted L = L \left( 1 - 0.89434e^{-0.61662 \left( \frac{L'}{L} \right)^{1.04831}} \right) \quad (7)$$

where  $L'$  = slab size (smaller dimension of a rectangular slab, length or width). This procedure also has limitations: (1) it considers only a single slab with no load transfer to adjacent slabs, and (2) it assumes a square slab. The square slab assumption is considered to produce sufficiently accurate results when the smaller dimension of a rectangular slab is assumed as  $L'$  (Darter et al. 1995). Darter et al. 1995 suggested using  $L' = \sqrt{Length \times Width}$  to further refine slab size corrections. However, no established procedures for correcting for load transfer to adjacent slabs have been reported so accounting for load transfer remains as a limitation of this method.

AASHTO (1993) suggests dividing the  $k_{FWD-Dynamic}$  value by a factor of 2 to determine the equivalent  $k_{FWD-Static}$  value. The origin of this factor 2 dates back to Foxworthy's work in the 1980s. Foxworthy (1985) reported comparisons between the  $k_{FWD-Dynamic}$  values obtained using Dynatest model 8000 FWD and the Static  $k$  values (Static  $k_{PLT}$ ) obtained from 30 in. diameter plate load tests (the exact procedure followed to calculate the Static  $k_{PLT}$  is not reported in Foxworthy 1985). Foxworthy used the AREA based back calculation procedure using the ILLI-SLAB finite element program. Results obtained from Foxworthy's study (Figure 24) are based on 7 FWD tests conducted on PCC pavements with slab thicknesses varying from about 10 in. to 25.5 in. and plate load tests conducted on the foundation layer immediately beneath the pavement over a 4 ft x 5 ft test area. A few of these sections consisted of a 5 to 12 in. thick base course layer and some did not. The subgrade layer material consisted of CL soil from Sheppard Air Force Base in Texas, SM soil from Seymour-Johnson Air Force Base in North Carolina, and an unspecified soil type from McDill Air Force base in Florida. No slab size correction was performed on this dataset.

Data from Foxworthy (1985) yielded a logarithmic relationship between the dynamic and the static  $k$  values. On average, the  $k_{FWD-Dynamic}$  values were about 2.4 times greater than the Static  $k_{PLT}$  values. Darter et al. (1995) indicated that the factor 2 is reasonable based on results from other test sites (Figure 24). Darter et al. (1995) also compared FWD test data from eight long-term pavement performance (LTPP) test sections with the Static  $k_{PLT}$  values and reported factors ranging from 1.78 to 2.16, with an average of about 1.91. The  $k_{FWD-Dynamic}$  values used in that comparison were corrected for slab size. For the analysis conducted in this research project, the corrected  $k_{FWD-Dynamic}$  values (for finite slab size) were divided by 2 and are reported as  $k_{FWD-Static-Corr}$  values.

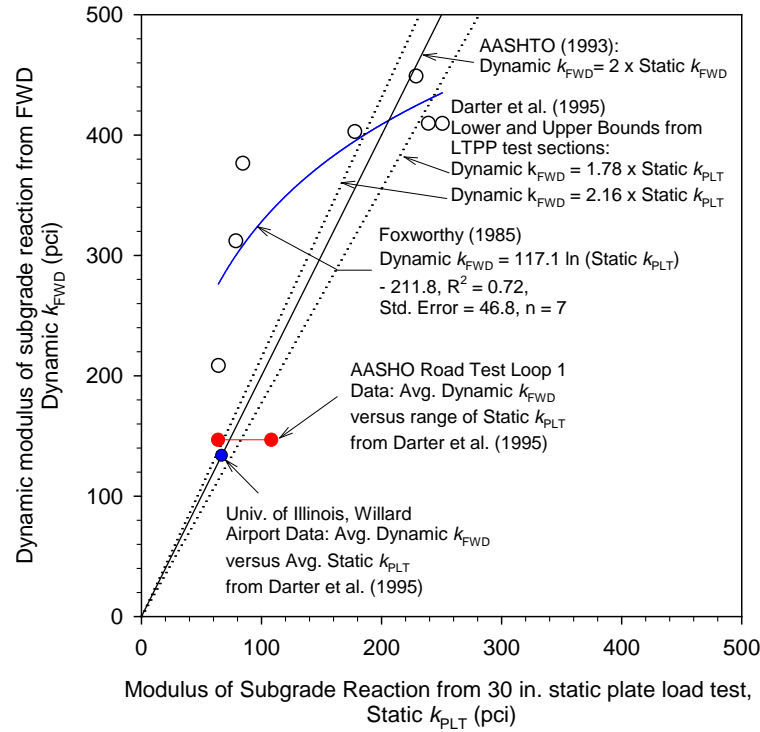


**Figure 24. Static  $k_{PLT}$  values versus  $k_{FWD}$ -Dynamic measurements reported in literature**

### Dynamic Cone Penetrometer

DCP tests were performed in accordance with ASTM D6951 (2003) to determine dynamic penetration index (DPI) in units of mm/blow and calculate California bearing ratio (CBR) using Equation 8.

$$CBR = \frac{292}{DPI^{1.12}} \quad (8)$$

Tests were conducted down to a depth of about 2m below pavement surface, by drilling a 20 mm hole in the pavement down to the top of the underlying base layer. The DCP test results are presented as CBR with depth profiles and as point values of  $CBR_{SB}$  representative of the subbase layer and  $CBR_{SG}$  representative of the top 305 mm of the subgrade. The top 305 mm of the subgrade was selected as the subgrade layer as it is typically the thickness used to scarify and recompact the material during construction. The point data values represent the weighted average CBR within each layer.

All DCP-CBR profiles were also reviewed to determine “weak” layers within the subgrade down to the bottom of the profile. An average CBR of a minimum of 75.6 mm (3 in.) thick layer within the top 1.5 m of subgrade (represented as  $CBR_{SG-Weak}$ ) was also calculated. The  $CBR_{SG-Weak}$  was determined to assess if weak layer would have influence on the  $k$  values determined using the FWD test.



The  $CBR_{SG}$  and  $CBR_{SG-Weak}$  values were converted to  $M_{r-SG}$  and  $M_{r-SG-Weak}$  of subgrade using nomograph provided in AASHTO (1993) as shown in Appendix A.

AASHTO (1993) uses the following empirical relationship to convert  $M_r$  to  $k$  value, where  $k$  is in units of kPa/mm and  $M_r$  is in units of MPa:

$$k = 2.03M_r \quad (8)$$



**Figure 25. In situ testing procedures: Kuab FWD setup with 300 mm diameter loading plate (a) and DCP with 2m extension rods (b)**

### **Pavement Condition Index**

Pavement condition index (PCI) testing was provided by the Iowa DOT based on testing conducted in 2011 (Iowa DOT 2014). PCI is a numerical indicator that rates the surface condition of the pavement based on distresses observed on the surface of the pavement but reflect structural capacity. PCI is commonly used as a rational basis for determining maintenance and repair needs. Field distress measurements are entered into PAVER™ 6.5, an inventory management software developed by the United States Army Corps of Engineers, Construction Engineering Research Laboratory. Pavement ratings based on PCI values are shown in Figure 26.

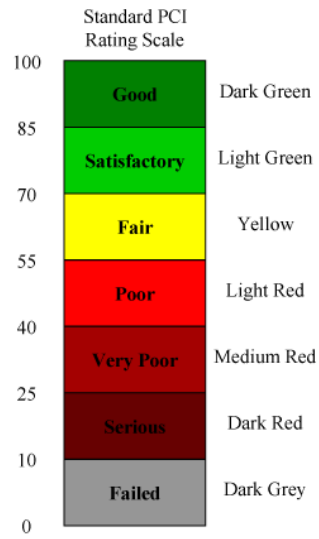


**Figure 26. PCI rating scale used in PAVER™ 6.5**

## CHAPTER 4. IN SITU TEST RESULTS

Pictures of the test sections from multiple site visits, raw FWD data plots, and raw DCP data plots from multiple site visits are provided in Appendices B to D, respectively. Analysis of the test results in terms of key measurement properties, comparisons between the test sites, and with the design assumed values are provided below.

### Seasonal Variations in Mechanistic Properties

Pavement temperature data was continuously (every hour) monitored at the Plainfield test site from the surface to about 1.2 m below the surface. Using the temperature data, 0° frost isotherms that form the boundaries of zones of frozen layers were estimated for two winters as shown in Figure 27a. Results indicate that the freezing period in 2010–11 lasted for about 3.5 months and in 2011–12 lasted for about 2.5 months. Thawing periods for the two seasons lasted for about 0.3–0.5 months. The maximum frost penetrations based on isotherms were around 1.2 and 0.6 m for 2010–11 and 2011–12 seasons, respectively. The number of freeze thaw cycles during the 2010–2011 winter are shown in Figure 28). The data shows that the upper 0.3 m of the pavement foundation was subjected to approximate 10 to 46 freeze-thaw cycles and the number of freeze-thaw cycles decreased to less than three at depths > 0.3 m.

FWD test results obtained from the Plainfield site are shown in Figure 27b and Figure 27c. The  $D_0$  and  $k_{\text{FWD-Static-Corr}}$  varied with variations in ground temperatures, as expected. During frozen conditions,  $D_0$  values were about 45% lower than values before freezing. During the thawing period, the  $D_0$  values were about the same as the values before freezing. After the thawing period, the  $D_0$  values recovered to levels that were similar to before freezing levels and remained relatively constant in the summer.

During frozen conditions, the  $k_{\text{FWD-Static-Corr}}$  values were nearly twice as higher than the values before freezing (Figure 27c). During the thawing period, the  $k_{\text{FWD-Static-Corr}}$  values dropped to the same level as before freezing and remained relatively constant during summer. Under thawing and summer conditions, the measured  $k_{\text{FWD-Static-Corr}}$  values were slightly lower than the Iowa DOT design  $k$  value (41 kPa/mm).

The  $k_{\text{FWD-Static-Corr}}$  values from all sites are presented in Figure 28, in comparison with the CBR values in the subbase ( $\text{CBR}_{\text{SB}}$ ) and subgrade layers ( $\text{CBR}_{\text{SG}}$  and  $\text{CBR}_{\text{SG-Weak}}$ ). The full-depth DCP-CBR profiles from the five test sites from three selected testing times are shown in Figure 30: February 2011 (frozen state), March 2011 (thawed state), and August 2011 (summer). Average  $k_{\text{FWD-Static-Corr}}$  values from each test site (based on 7 to 8 tests) and  $\text{CBR}_{\text{SB}}$ ,  $\text{CBR}_{\text{SG}}$ , and  $\text{CBR}_{\text{SG-Weak}}$  values are presented as bar charts for measurements obtained in each season (frozen, thawed, and summer) in Figure 31, for comparison between test sites and seasons. The Fort Dodge, Denison, Merville, and Nevada test sites are within 200 miles of the Plainfield site and are in the same climatic zone. Due to lack of temperature data from each site, the time of thawing and freezing is assumed to be the same at all sites for analysis in this paper, although some variations are expected between the test sites.

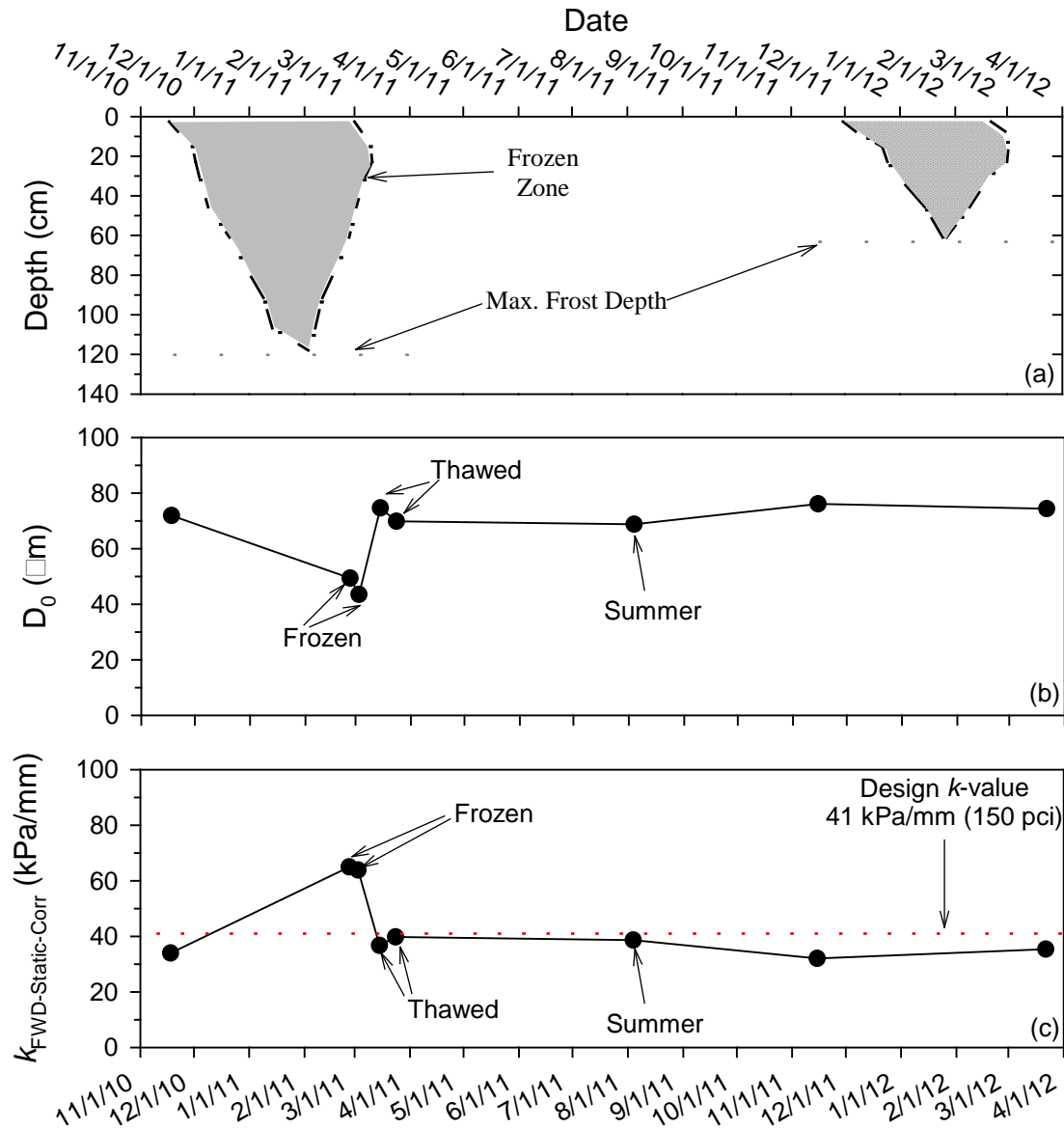


**Figure 27.  $0^\circ$  isotherm with time (a), seasonal variations of  $D_0$  (b), and seasonal variations of  $k_{FWD-Static-Corr}$  (c) at the Plainfield test site**

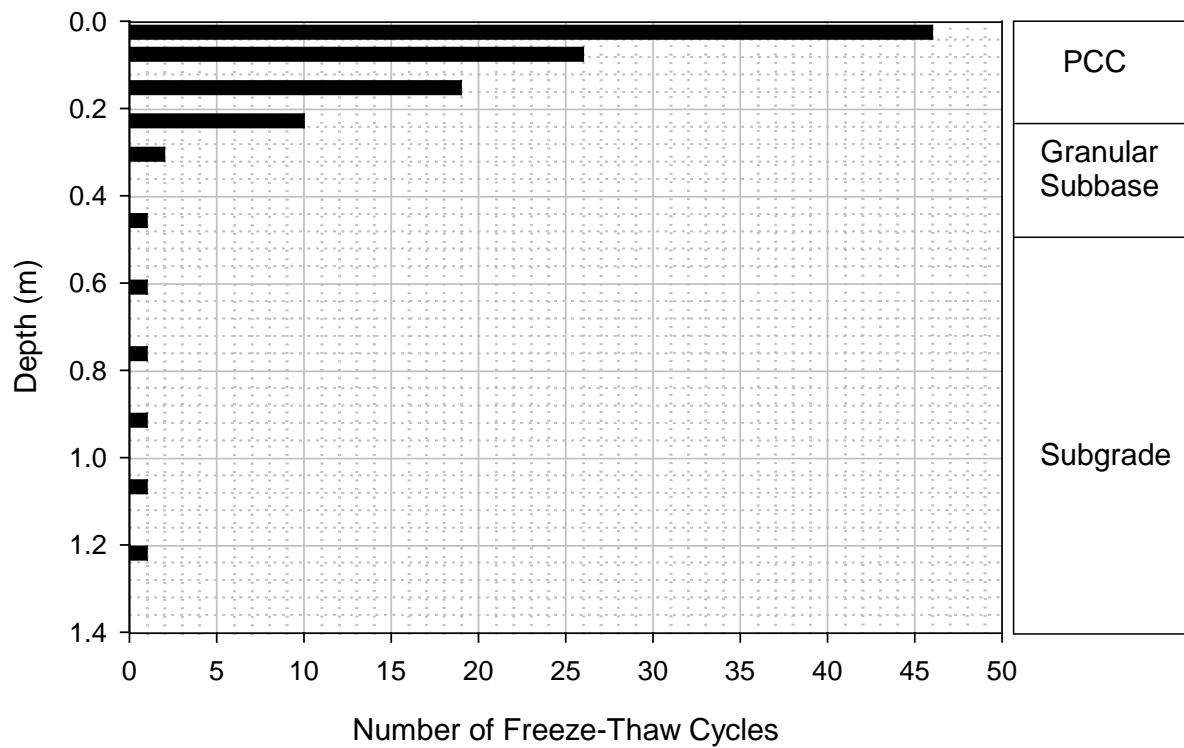


**Figure 28. Number of freeze-thaw cycles versus depth during winter 2010–2011 at US Highway 218 near Plainfield, Iowa**

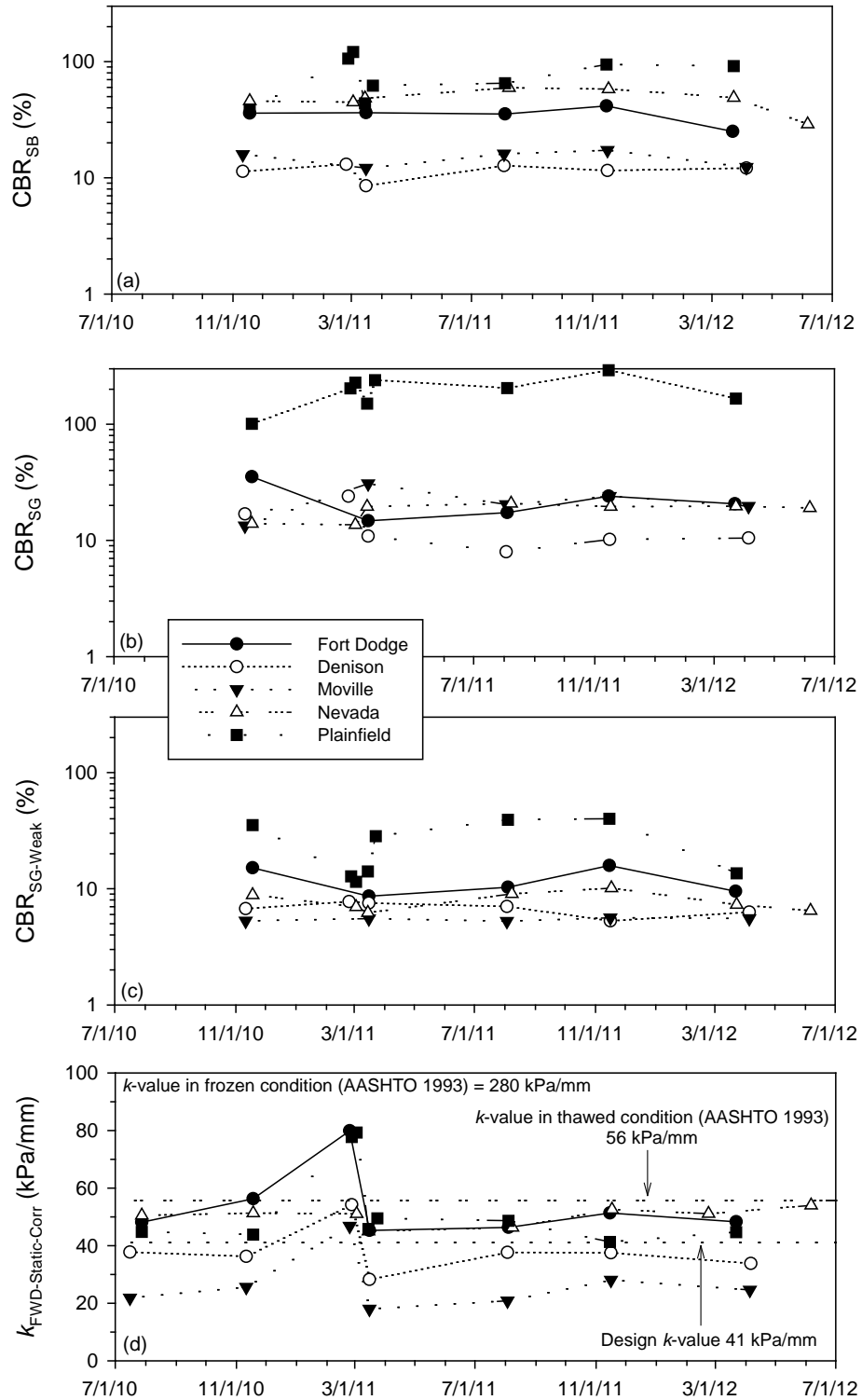


**Figure 29. Seasonal variations in mechanistic properties at the five test sites:  $CBR_{SB}$  (a)  $CBR_{SG}$  (b),  $CBR_{SG-Weak}$  (c), and  $k_{FWD-Static-Corr}$  (d)**

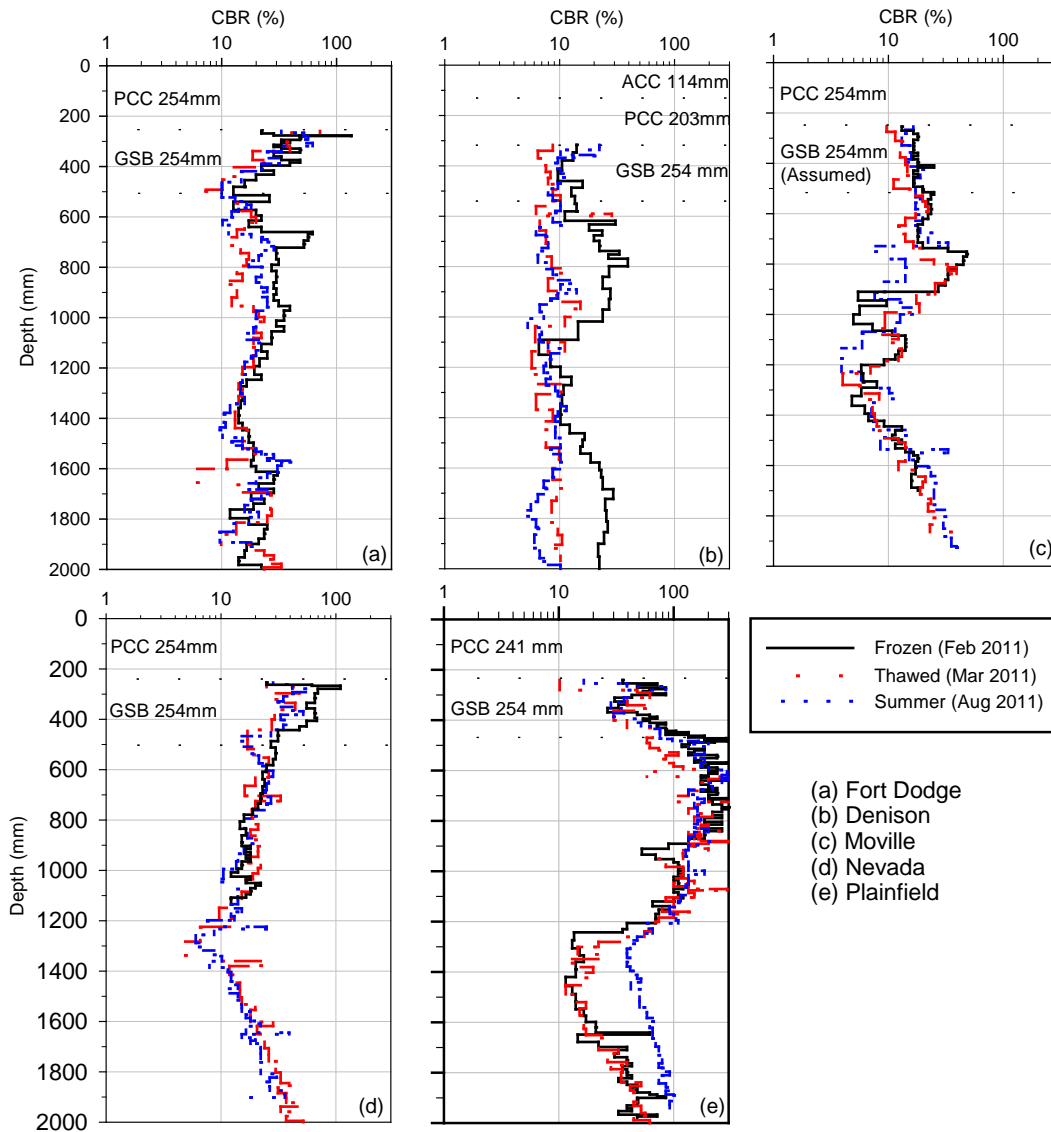


**Figure 30. DCP-CBR profiles at the five test sites in February (frozen state), March (thawed state), and August (summer)**

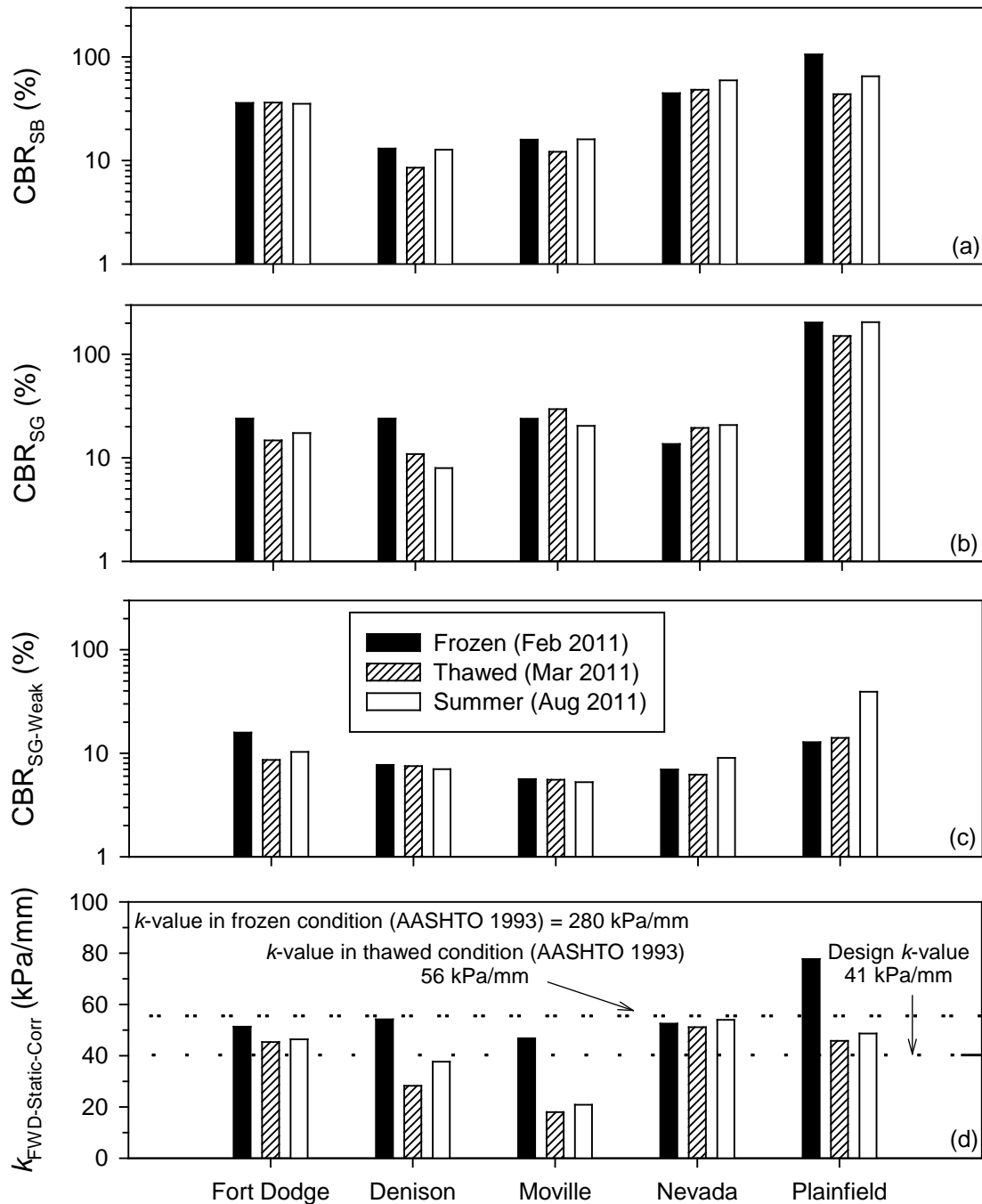


**Figure 31. Summary of seasonal changes in  $CBR_{SB}$  (a),  $CBR_{SG}$  (b),  $CBR_{SG-Weak}$  (c), and  $k_{FWD-Static-Corr}$  (d) at each site**

On average, there was no significant difference in  $k_{FWD-Static-Corr}$  values obtained in thawed condition and summer at any of the sites. The CBR values also did not show significant differences between thawed condition and summer at most of the sites, except at the Plainfield site where  $CBR_{SG-Weak}$  increased from about 10 in thawed state to about 40 in summer. The



$k_{\text{FWD-Static-Corr}}$  values in frozen condition was about 10% to 56% higher than in summer at four of the five sites. At the Nevada test site, the values were about the same at all testing times.

At two of the five sites, the  $k_{\text{FWD-Static-Corr}}$  values were about 1.5 to 2 times lower than the design assumed  $k$  value (41 kPa/mm) in thawed condition and in summer.

### Empirical Relationships between $k$ , $M_r$ , and CBR Values

CBR data obtained from this study was converted to  $M_r$  values based on empirical relationships provided in AASHTO (1993). AASHTO (1993) uses a simple empirical model to convert  $M_r$  to  $k$  for use in design as shown earlier in Equation 8.  $k$  values obtained from FWD testing are compared in Figure 32 with the  $M_r$  values and the CBR values, in reference to the AASHTO empirical model for  $k$ - $M_r$  and PCA (1984) model for CBR- $M_r$ . CBR and  $M_r$  values of the subgrade are presented for the average of the top 300 mm of the subgrade and the weak layer within the subgrade.

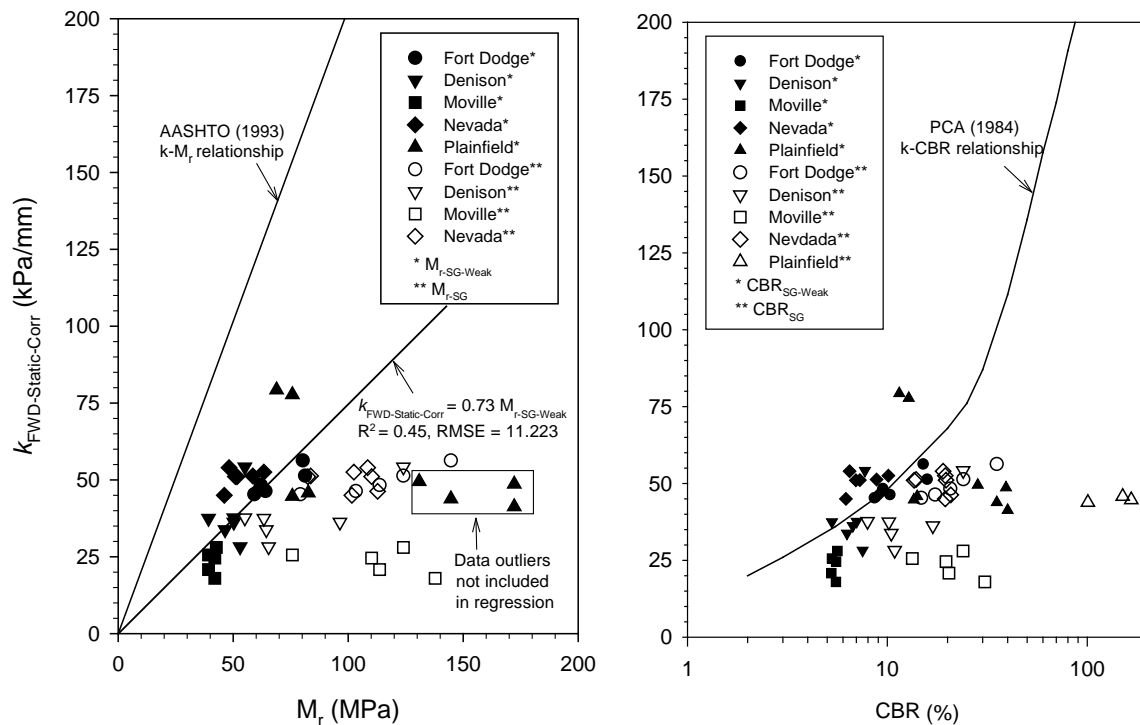


**Figure 32. Relationship between  $M_r$  values determined from CBR and  $k_{\text{FWD-Static-Corr}}$  compared with the relationship proposed in AASHTO (1993) (left) and relationship between CBR values and  $k_{\text{FWD-Static-Corr}}$  compared with the relationship proposed in PCA (1984)**

Results indicated that the  $M_{r\text{-SG}}$  and the  $\text{CBR}_{\text{SG}}$  values were unrealistically high.  $M_{r\text{-SG-Weak}}$  and  $\text{CBR}_{\text{SG-Weak}}$  were much lower. A simple linear regression fit was applied to  $M_{r\text{-SG-Weak}}$  versus  $k_{\text{FWD-Static-Corr}}$  results, which yielded a coefficient of determination ( $R^2$ ) of 0.45 with root mean

square error (RMSE) of 11.2 kPa/mm for  $k$  values. Compared to the linear regression fit in the data, use of the AASHTO model significantly over estimated the  $k$  values. A best fit regression line was not found for the  $k$ -CBR data.

It is important for designers and practitioners to recognize the uncertainties in estimated values based on empirical relationships and to note the differences that exist between values calculated from results of different test methods. Also, it must be noted that  $k$  and  $M_r$  are stress-dependent parameters and that most of the empirical relationships between CBR vs.  $M_r$  and  $M_r$  vs.  $k$  do not properly address this issue.

### **Mechanistic Properties versus Pavement Performance**

The pavement ride quality data available for each test section (PCI) is compared in relationship with pavement age, and in situ test measurements  $k_{\text{FWD-Static-Corr}}$  and  $\text{CBR}_{\text{SG-Weak}}$  in Figure 33 and Figure 34. The relationship between pavement age and PCI showed a strong linear trend with  $R^2 > 0.93$ . A similar linear regression relationship was documented by White and Vennapusa (2014) based on tests conducted on low volume jointed PCC pavement test sites.

The relationship between  $k_{\text{FWD-Static-Corr}}$  and PCI also yielded a strong linear regression relationship with  $R^2 > 0.95$ , while the relationship between  $\text{CBR}_{\text{SG-Weak}}$  and PCI yielded a strong non-linear exponential trend with PCI with  $R^2 > 0.95$ . These trends suggest that higher foundation layer stiffness or strength provides a better ride quality and that pavement age also influences ride quality.

White and Vennapusa (2014) also conducted multivariate statistical analysis on various parameters measured from their study to predict PCI. The parameters are shown in the prediction equation provided in Figure 33. The prediction equations suggests that by improving subgrade strength/stiffness (within about top 16 in. of the subgrade layer), improving drainage, providing a subbase layer, and reducing variability, the PCI value can potentially be improved. White and Vennapusa (2014) suggested that subgrade layer properties can be improved by stabilization, drainage can be improved by the presence of a relatively thin drainable subbase layer (note that subbase layer thickness was not statistically significant), and variability can be reduced by adequate in situ testing. It is important to note that the PCI prediction model is based on limited data (16 points) and must be validated with a larger pool of data.

Although additional testing is warranted to further explore and validate these empirical models, an advantage these models is that designers can use them to control the mechanistic properties of foundation layer and target a desired ride quality for a target design age.

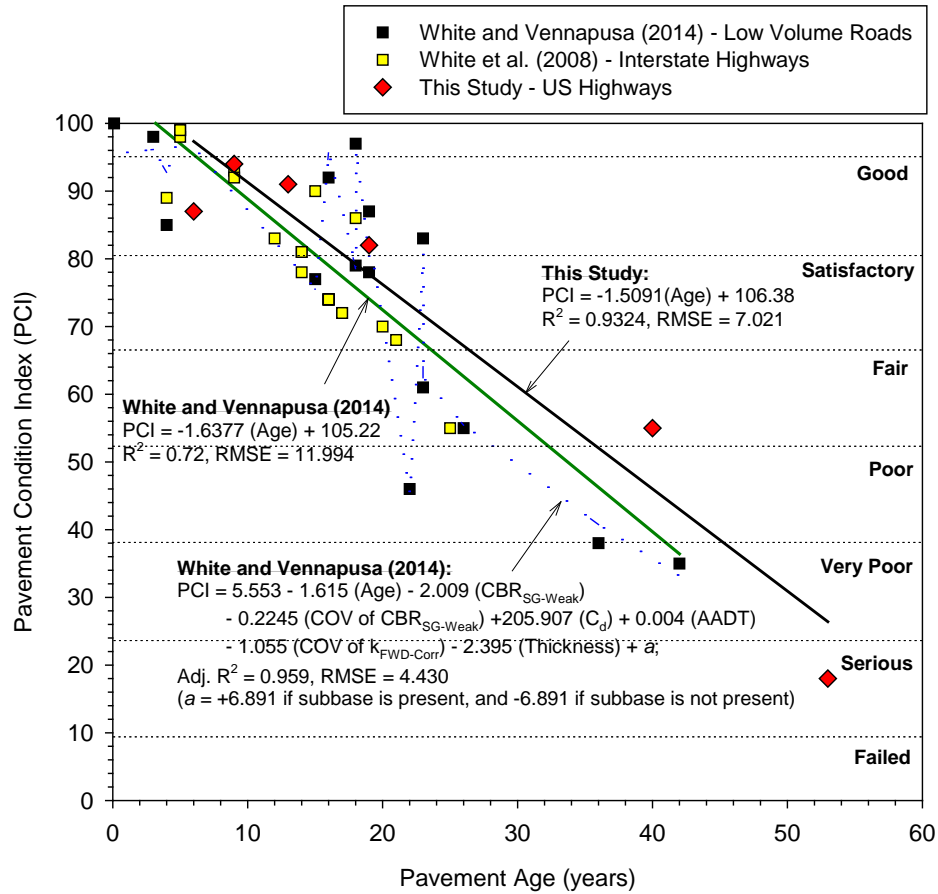


**Figure 33. PCI versus pavement age from this study in comparison with results presented in White and Vennapusa (2012) and White et al. (2008)**

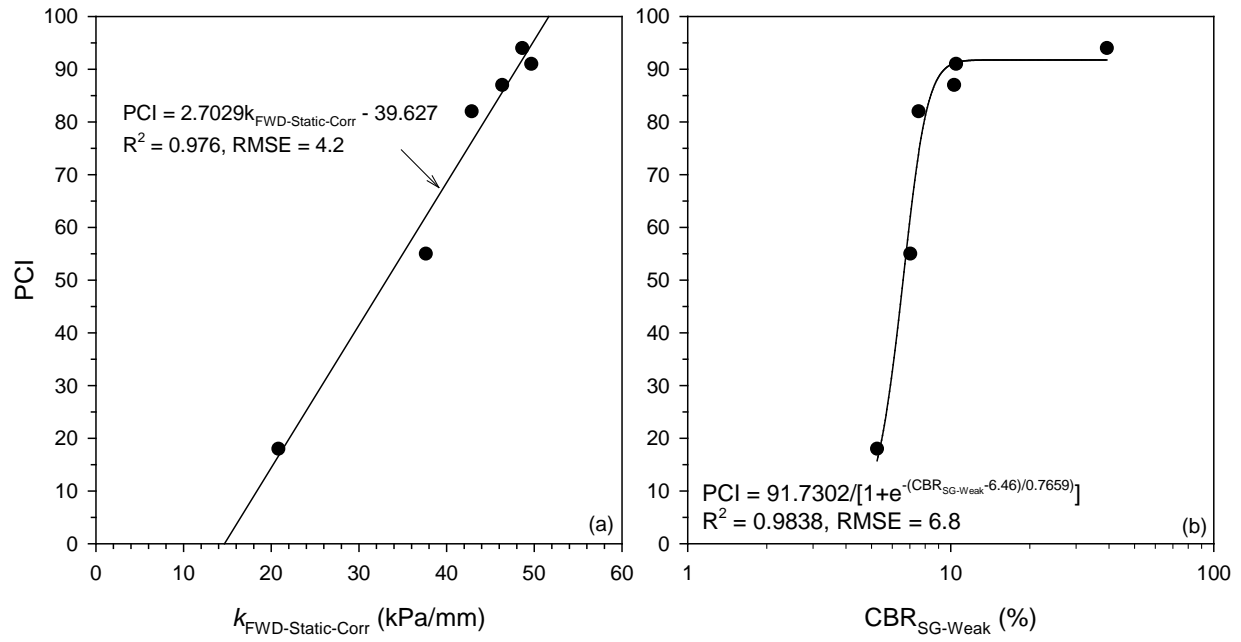


**Figure 34. PCI versus  $k_{\text{FWD-Static-Corr}}$  (left) and  $\text{CBR}_{\text{SG-Weak}}$  (right)**

## CHAPTER 5. SUMMARY OF KEY FINDINGS

Following are some key findings from this study:

- On average, there was no significant difference in  $k_{\text{FWD-Static-Corr}}$  values obtained in thawed condition and summer at any of the sites. The CBR values also did not show significant differences between thawed condition and summer at most of the sites, except at the Plainfield site where  $\text{CBR}_{\text{SG-Weak}}$  increased from about 10 in thawed state to about 40 in summer. The  $k_{\text{FWD-Static-Corr}}$  values in frozen condition was about 10% to 56% higher than in summer at four of the five sites. At one test site, the values were about the same at all testing times.
- At two of the five sites, the  $k_{\text{FWD-Static-Corr}}$  values were about 1.5 to 2 times lower than the design assumed  $k$  value (41 kPa/mm) in thawed condition and in summer.
- Results indicated that the  $M_{\text{r-SG}}$  values were unrealistically high when compared with the  $k_{\text{FWD-Static-Corr}}$ .  $M_{\text{r-SG-Weak}}$  were much lower than the  $M_{\text{r-SG}}$  values. A simple linear regression fit was applied to  $M_{\text{r-SG-Weak}}$  versus  $k_{\text{FWD-Static-Corr}}$  results, which yielded a  $R^2$  of 0.45 with RMSE of 11.2 kPa/mm for  $k$  values. Compared to the linear regression fit in the data, use of the AASHTO model significantly over estimates the  $k$  values.
- It is important for designers and practitioners to recognize the inherent uncertainty in estimated values when using empirical relationships and further to recognize the differences that exist between the values calculated from different test methods. Also, it must be noted that  $k$  and  $M_{\text{r}}$  are stress-dependent parameters and most of the empirical relationships between CBR vs.  $M_{\text{r}}$  and  $M_{\text{r}}$  vs.  $k$  do not properly address this issue.
- The relationship between pavement age and PCI showed a strong linear trend with  $R^2 > 0.93$ . A similar linear regression relationship was documented by White and Vennapusa (2014) based on testing on low volume jointed PCC pavement test sites.
- The relationship between  $k_{\text{FWD-Static-Corr}}$  and PCI yielded a strong linear regression relationship with  $R^2 > 0.95$ , while the relationship between  $\text{CBR}_{\text{SG-Weak}}$  and PCI yielded a strong non-linear exponential trend with PCI with  $R^2 > 0.95$ . These trends suggest that higher foundation layer stiffness or strength provide a better ride quality and that ride quality is influenced by pavement age. Although additional testing is warranted to further explore and validate these empirical models, an advantage of having these models is that designers can use them to target a desired ride quality for a target design age by controlling foundation layer mechanistic properties.



## REFERENCES

- AASHTO (1993). Guide for Design of Pavement Structures. American Association of State Highway and Transportation Officials, Washington, D.C.
- AASHTO (2008). Mechanistic-Empirical Pavement Design Guide: A Manual of Practice. 2nd Edition. American Association of State Highway and Transportation Officials, Washington, D.C.
- Andersland, O.B., and Ladanyi, B. (2004). Frozen ground engineering, 2nd Ed., John Wiley and Sons, Inc., NJ.
- ASTM D-6951. (2003). "Standard Test Method for Use of the Dynamic Cone Penetrometer in Shallow Pavement Applications." ASTM International, West Conshohocken, PA.
- ASTM D-4694. (2009). "Standard Test Method for Deflections with a Falling-Weight-Type Impulse Load Device." ASTM International, West Conshohocken, PA.
- Baladi, G., Dawson, T., and Sessions, C. (2009). Pavement Subgrade MR Design Values for Michigan's Seasonal Changes. Final Report, RC-1531. Michigan Department of Transportation.
- Barenberg, E. J., and Petros, K. A. (1991). Evaluation of Concrete Pavements Using NDT Results, Illinois Highway Research Project IHR-512, University of Illinois and Illinois Department of Transportation, Report No. UILU-ENG-91-2006, IL.
- Becker, P. J., White, D. J., Vennapusa, P. K. R., and Dunn, M. J. (2014). "Freeze-Thaw Performance Assessment of Stabilized Pavement Foundations." Transportation Research Board, 93rd Annual Meeting, January 12–16, 2014, Washington, D.C.
- Brandl, H. (2008). "Freezing-thawing behavior of soils and unbound road layers." Slovak Journal of Civil Engineering, 2008/3: 4–12.
- Casagrande, A., Taber, S., and Watkins, W. (1931). "Discussion of Frost Heaving." Highway Research Board Proceeding, Vol. 11, 165–177.
- Crovetti, J. A. (1994). "Evaluation of jointed concrete pavement systems incorporating open-graded bases." Ph.D. Dissertation, University of Illinois at Urbana-Champaign, IL.
- Darter, M. I., Hall, K. T., and Kuo, C-M. (1995). Support under Portland Cement Concrete Pavements, NCHRP Report 372. Transportation Research Board, Washington, D.C.
- Deblois, K., Bilodeau, J., and Dore, G. (2010). "Use of falling weight deflectometer time history data for the analysis of seasonal variation in pavement response." Canadian Journal of Civil Engineering, 37: 1224–1231 (2010). DOI:10.1139/L10-069.
- Drumm, E. C. and Meier, R.W. (2003) "LTPP Data Analysis: Daily and Seasonal Variations in In Situ Material Properties, Project 20-50(7&12)" Final Report to National Cooperative Highway Research Program, <[http://trb.org/publications/nchrp/nchrp\\_w60.pdf](http://trb.org/publications/nchrp/nchrp_w60.pdf)>.
- ERES Consultants Inc. (1982). Techniques for Pavement Rehabilitation: A Training Course. U.S. Department of Transportation, FHWA, Washington, D.C.
- Hoffman, M. S., and Thompson, M. R. (1981). Mechanistic Interpretation of Nondestructive Pavement Testing Deflections. Transportation Engineering Series No. 32, Illinois cooperative Highway and Transportation Research Series No. 190. University of Illinois at Urbana-Champaign, Champaign, IL.
- Hoover, J. M., Huffman, R. T., and Davidson, D. T. (1962). "Soil stabilization field trials, primary Highway 117, Jasper Country, Iowa." The Forty First Annual Meeting of the Highway Research Board, NAS-NRC, Washington D.C., January 1962.

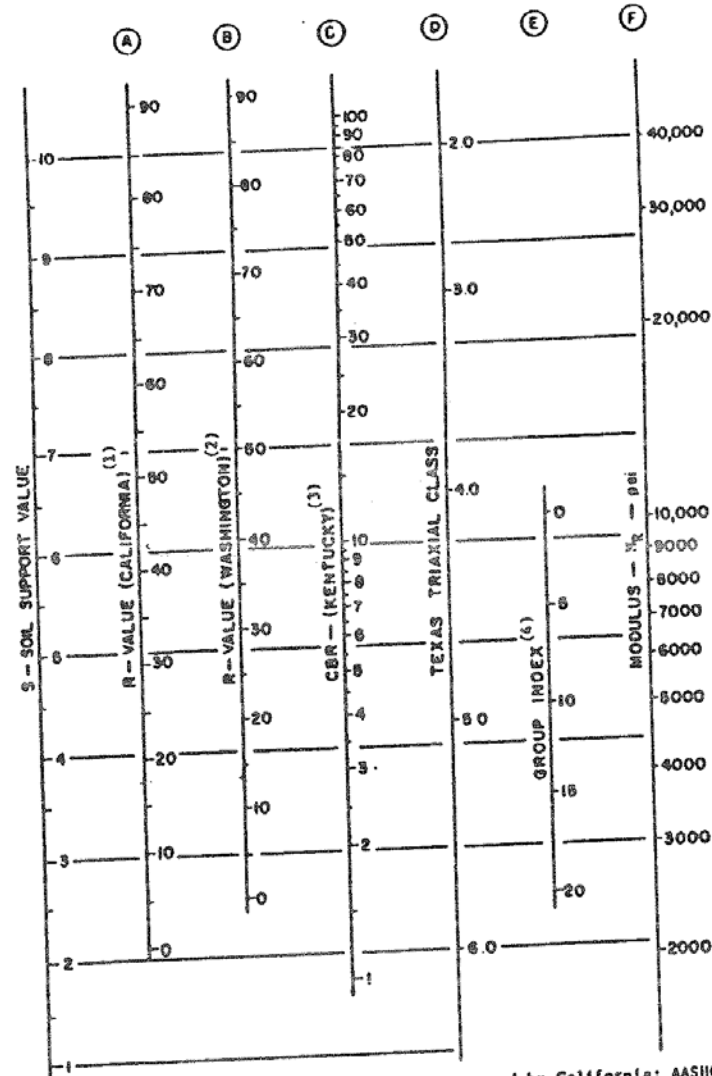
- Ioannides, A. M. (1990). "Dimensional analysis in NDT rigid pavement evaluation." *Transportation Engineering Journal*, ASCE, Vol. 116, No. TE1.
- Iowa DOT. (2014). Test Sections by Milepost – Primary. Special Investigations Office of Materials Highway Division, Iowa Department of Transportation.
- Iowa State Environmental Mesonet (2012). RWIS Soil Probe Download. Iowa State University Department of Agronomy. Accessed October 5, 2012.  
<http://mesonet.agron.iastate.edu/request/rwis/soil.phtml>.
- Janoo, V. C., and Berg, R. L. (1996). PCC Airfield Pavement Response during Thaw-Weakening Periods – A Field Study. Special Report 96-12. CRREL, US Army Corps of Engineers.
- Janoo, V. C., and Berg, R. L. (1998). "PCC Airfield Pavement Response during Thaw-Weakening Periods." *Journal of Cold Regions Engineering*. Vol. 12, No. 3.
- Janoo, V. C., and Shepherd, K. (2000). "Seasonal Variation of Moisture and Subsurface Layer Moduli." *Transportation Research Record* 1709. No. 00-0929.
- Janssen, D. J., and Snyder, M. B. (2000). "Temperature-moment concept for evaluating pavement temperature data." *Journal of Infrastructure Systems*, 6(2), 81–83.
- Johnson, A. (2012). "Freeze-thaw performance of pavement foundation materials." M.S. Thesis. Iowa State University. Ames, Iowa.
- Joint Departments of the Army and Air Force USA. (1985). Pavement Design for Seasonal Frost Conditions. Technical Manual TM 5–818–2/AFM 88–6, Chapter 4. Washington, D.C. U.S. Government Printing Office.
- Konrad, J-M, and Roy, M. (2000). "Flexible pavement in cold regions: a geotechnical perspective." *Can. Geotech. J.* 37: 689–699 (2000).
- Lary, J. A., Mahoney, J. P., and Sharma, J. (1984). Evaluation of Frost Related Effects on Pavements. Final Report, WA-RD 67.1. Washington State Transportation Research Center and the University of Washington.
- Lukanen, E. O., Worel, B. J., and Clyne, T. (2006). "MnROAD Environmental Factors that Affect Ride." *Proceedings of the 13<sup>th</sup> International Conference on Cold Regions Engineering*. Ed. M. Davies, J.E. Zulfelt, July 23–26, Orono, Maine.
- McCracken, J. K. (2008). "Seasonal Analysis of the Response of Jointed Plain Concrete Pavements to FWD and Truck Loads." MS, University of Pittsburg, Pittsburg, PA.
- Newcomb, D. E., and Birgisson, B. (1999). NCHRP Synthesis of Highway Practice 278: Measuring In Situ Mechanical Properties of Pavement Subgrade Soils. Transportation Research Board, National Research Council, Washington D.C., 1999. 43–51.
- NDDOT. (2015). "Why there are Spring Load Restrictions." North Dakota Department of Transportation. Accessed in December 10, 2015.  
<https://www.dot.nd.gov/divisions/maintenance/springldresticprocedures.htm>
- Orr, D. P. (2003). "Detection of Nonresilient Behavior in Pavements with a Falling-Weight Deflectometer." *Transportation Research Record* 1860. No. 03-3688.
- Ovik, J. M., Siekmeier, J. A., and Van Deusen, D. A. (2000). Improved Spring Load Restriction Guidelines Using Mechanistic Analysis. Final Report. 2000-18. Minnesota Department of Transportation.
- PCA. (1984). Thickness Design for Concrete Highway and Street Pavement. Portland Cement Association.
- Puppala, A. J. (2008). Estimating Stiffness of Subgrade and Unbound Materials for Pavement Design. NCHRP Synthesis 382. Transportation Research Board.



- Saarenketo, T., and Saara, A. (2005). *Managing spring thaw weakening on low volume roads – problem description, load restriction policies, monitoring and rehabilitation*. Final report 2\_3 Roadex II Project. Roadscanners.
- Salour, F., and Erlingsson, S. (2012). *Pavement structural behavior during spring thaw*. The Swedish National Road and Transport Research Institute, VTI Report 738A.
- Schmalzer, P. N. (2006). LTPP Manual for Falling Weight Deflectometer Measurements, Version 4.1. Final Report, FHWA-HRT-06-132. Federal Highway Administration.
- Simonsen, E., and Isacsson, U. (1999). “Thaw weakening of pavement structures in cold regions.” *Cold Regions Science and Technology*. 29(2), 135–151.
- Smith, K. D., Wade, M. J., Bruinsma, J. E., Chatti, K., Vandenbossche, J. M., Yu, H. T., Hoerner, T. E., Tayabji, S. D. (2007). Using Falling Weight Deflectometer Data with Mechanistic-Empirical Design and Analysis, Draft Interim Report, DTFH61-06-C-0046, Federal Highway Administration, Washington, D.C.
- Solanki, P., Zaman, M. and Khalife, R. (2013). “Effect of Freeze-Thaw Cycles on Performance of Stabilized Subgrade.” *Sound Geotechnical Research to Practice*, pp. 566-580.
- Stubstad, R. N., Jiang, Y. J., and Lukanen, E. O. (2006). Guidelines for Review and Evaluation of Backcalculation Results, FHWA-RD-05-152, Federal Highway Administration, Washington, D.C.
- Vennapusa, P. K. R. (2008). “Investigation of roller-integrated compaction monitoring and in-situ testing technologies for characterization of pavement foundation layers.” Ph.D. Thesis. Iowa State University. Ames, Iowa.
- White, D. J., Becker, P., Vennapusa, P. K. R., Dunn, M. J., and White, C. I. (2013). “Soil stiffness of stabilized pavement foundations.” *Transportation Research Record: Journal of the Transportation Research Board*. No. 2335, Transportation Research Board of the National Academies, Washington, D.C., 2013, pp. 99–109. DOI: 10.3141/2335-11
- White, D. J., and Vennapusa, P. K. R. (2014). Optimizing Pavement Base, Subbase and Subgrade Layers for Cost and Performance on Local Roads. Final Report. InTrans Project 11-422. Iowa State University. Ames, IA.
- Zhang, Y. (2015). “Laboratory freeze–thaw assessment of cement, fly ash, and fiber stabilized pavement foundation materials.” *Cold Regions Science and Technology*. 122 (2016) 50–57. DOI:10.1016/j.coldregions.2015.11.005

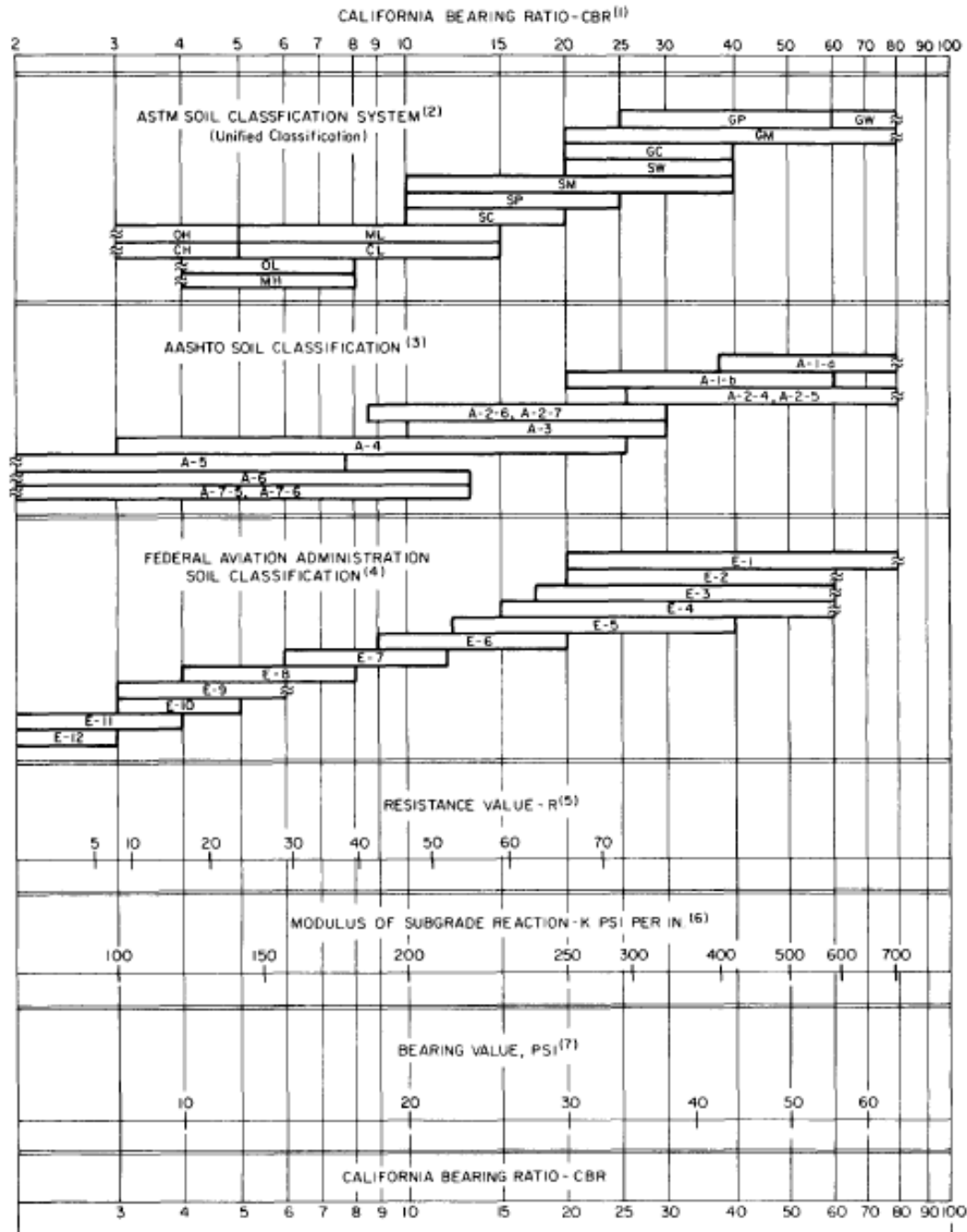


## APPENDIX A: AASHTO (1993) AND PCA (1984) DESIGN CHARTS



- (1) The correlation is with the design curves used by California; AASHTO designation is T-173-60, and exudation pressure is 240 psi. See Nveem, F.H., and Carmany, R.H., "The Factors Underlying the Rational Design of Pavements." *Proc. HRR*, Vol. 28 (1948) pp. 101-136.
- (2) The correlation is with the design curves used by Washington Dept. of Highways; exudation pressure is 300 psi. See "Flexible Pavement Design Correlation Study." *HRB Bull. 133* (1956).
- (3) The correlation is with the CRR design curves developed by Kentucky. See Drake, W.S., and Havens, J.H., "Re-Evaluation of Kentucky Flexible Pavement Design Criterion." *HRB Bull. 233* (1959) pp. 33-56. The following conditions apply to the laboratory-modified CRR: specimen is to be molded at or near the optimum moisture content as determined by AASHTO T-99; dynamic compaction is to be used with a hammer weight of 10 lb dropped from a height of 18 in.; specimen is to be compacted in five equal layers with each layer receiving 10 blows; specimen is to be soaked for 4 days.
- (4) This scale has been developed by comparison between the California R-value and the Group Index determined by the procedure in *Proc. HRR* Vol. 25 (1945) pp. 376-392.

Figure 35. Chart for estimating resilient modulus ( $M_r$ ) of subgrade from CBR (from AASHTO 1993 Appendix FF based on results from Til et al. 1972)



(1) For the basic idea, see O. J. Porter, "Foundations for Flexible Pavements," Highway Research Board Proceedings of the Twenty-second Annual Meeting, 1942, Vol. 22, pages 100-136.

(2) ASTM Designation D2487.

(3) "Classification of Highway Subgrade Materials," Highway Research Board Proceedings of the Twenty-fifth Annual Meeting, 1945, Vol. 25, pages 376-392.

(4) Airport Paving, U.S. Department of Commerce, Federal Aviation Agency, May 1948, pages 11-16. Estimated using values given in FAA Design Manual for Airport Pavements (Formerly used FAA Classification; Unified Classification now used.)

(5) C. E. Warnes, "Correlation Between  $R$  Value and  $k$  Value," unpublished report, Portland Cement Association, Rocky Mountain-Northwest Region, October 1971 (best-fit correlation with correction for saturation).

(6) See T. A. Middlebrooks and G. E. Bertram, "Soil Tests for Design of Runway Pavements," Highway Research Board Proceedings of the Twenty-second Annual Meeting, 1942, Vol. 22, page 152.

(7) See item (6), page 184.

**Figure 36. Chart for estimating modulus of subgrade reaction ( $k$ ) from CBR (from PCA 1984)**

## APPENDIX B: FWD TEST RESULTS

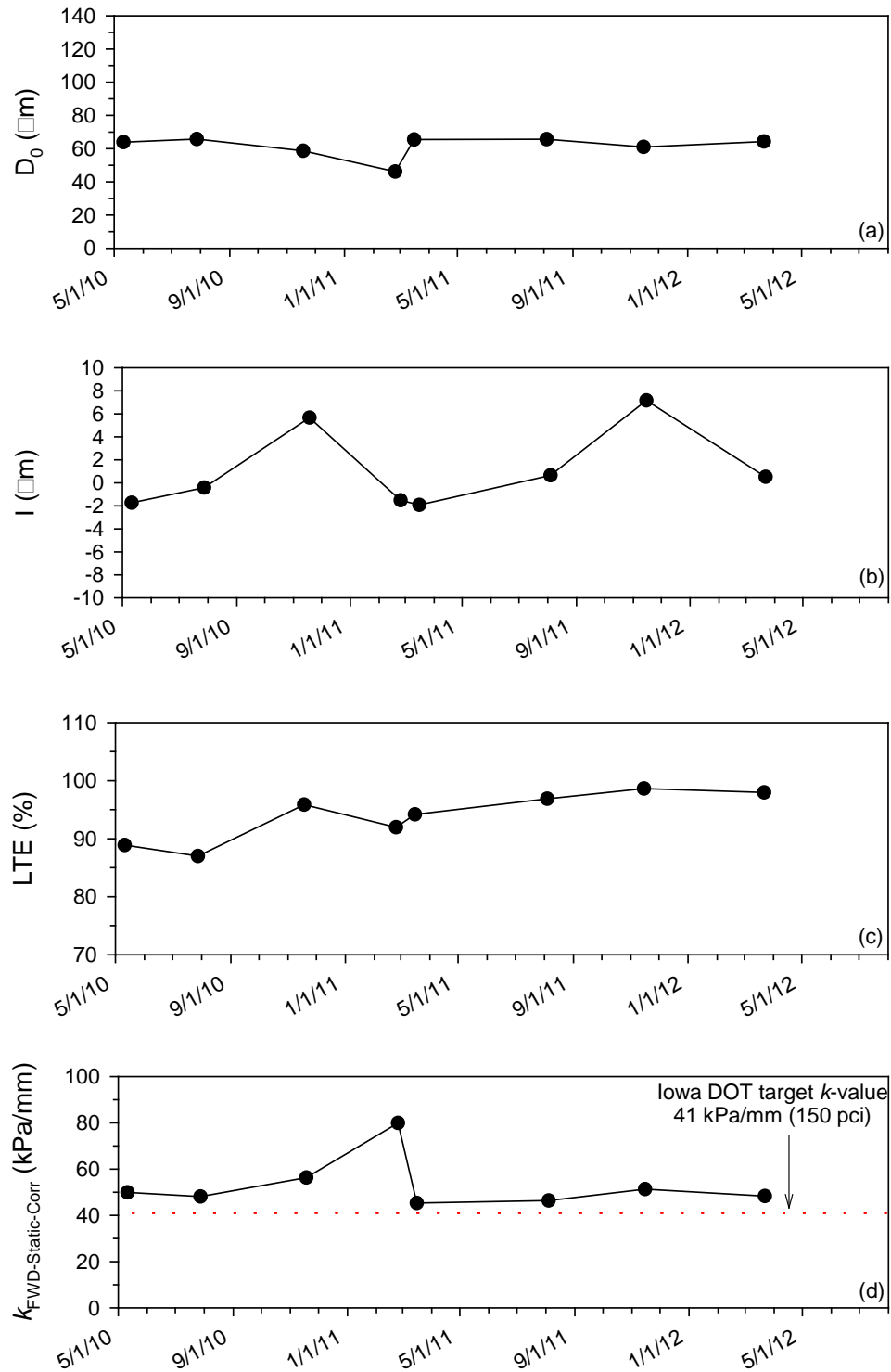
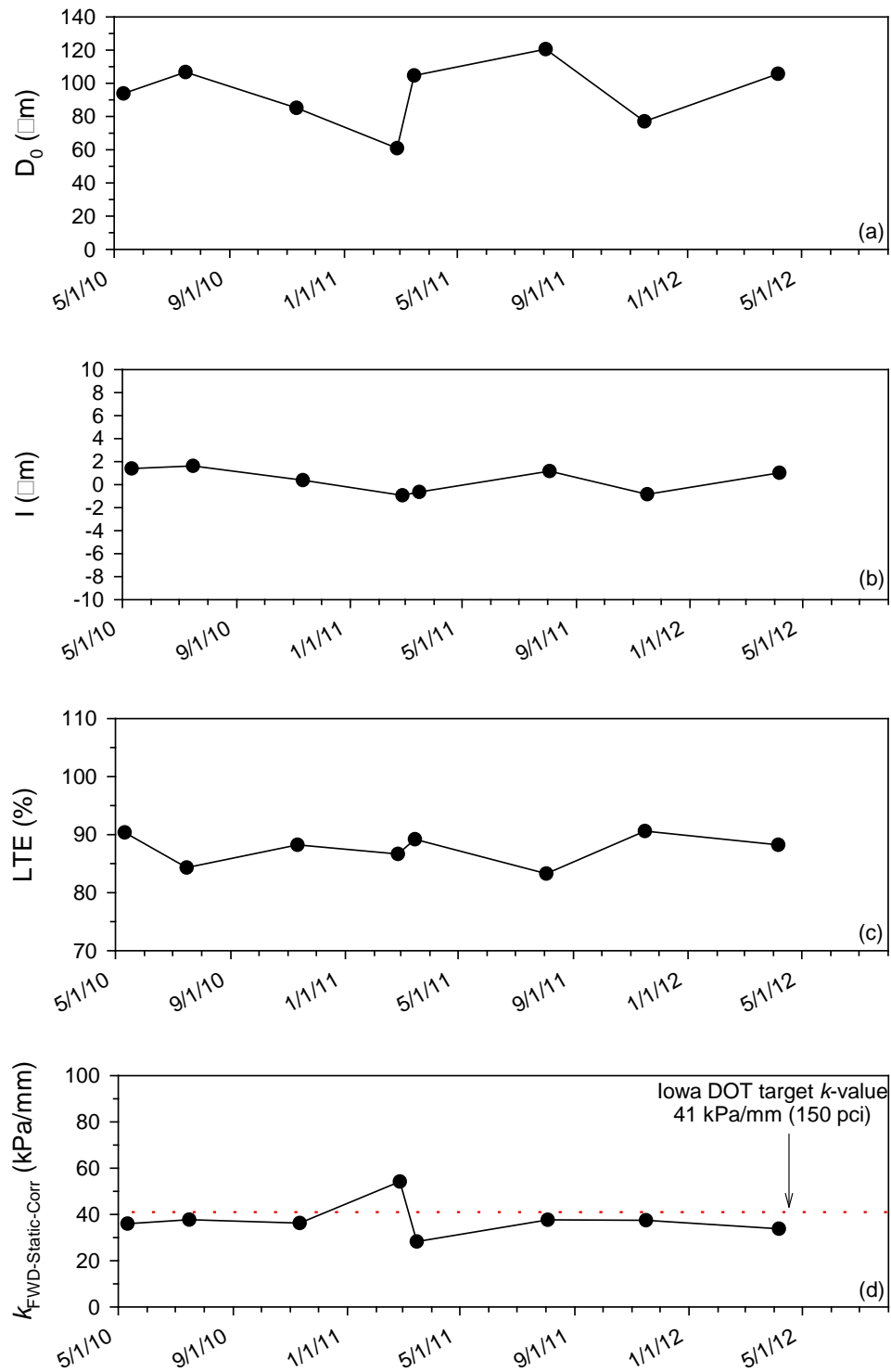
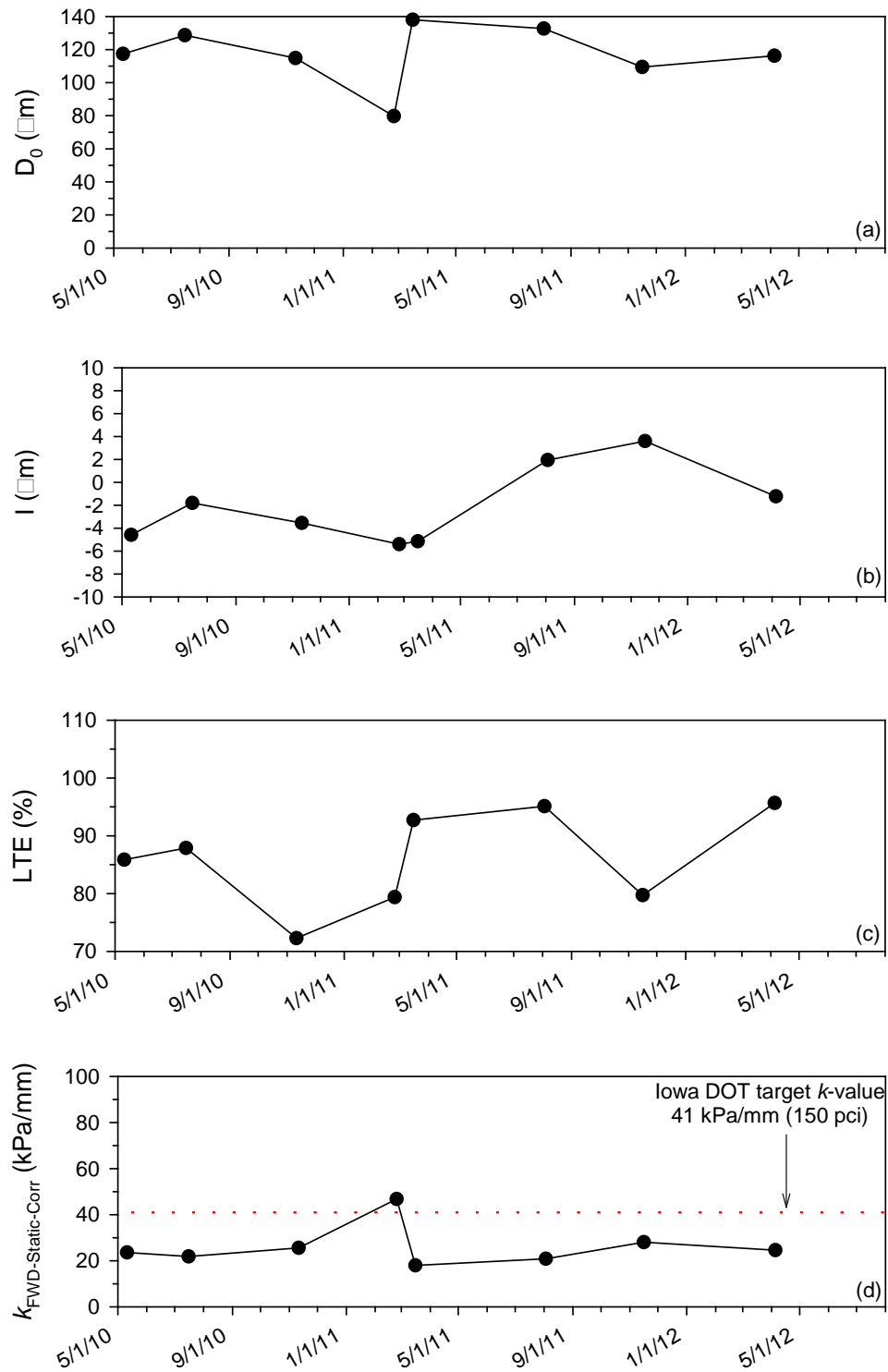


Figure 37. Seasonal FWD test results of US 20 WB near MP 18.5, Fort Dodge



**Figure 38. Seasonal FWD test results of US 59 NB near MP 95.0, Denison**



**Figure 39. Seasonal FWD test results of US 20 EB near MP 18.5, Moville**

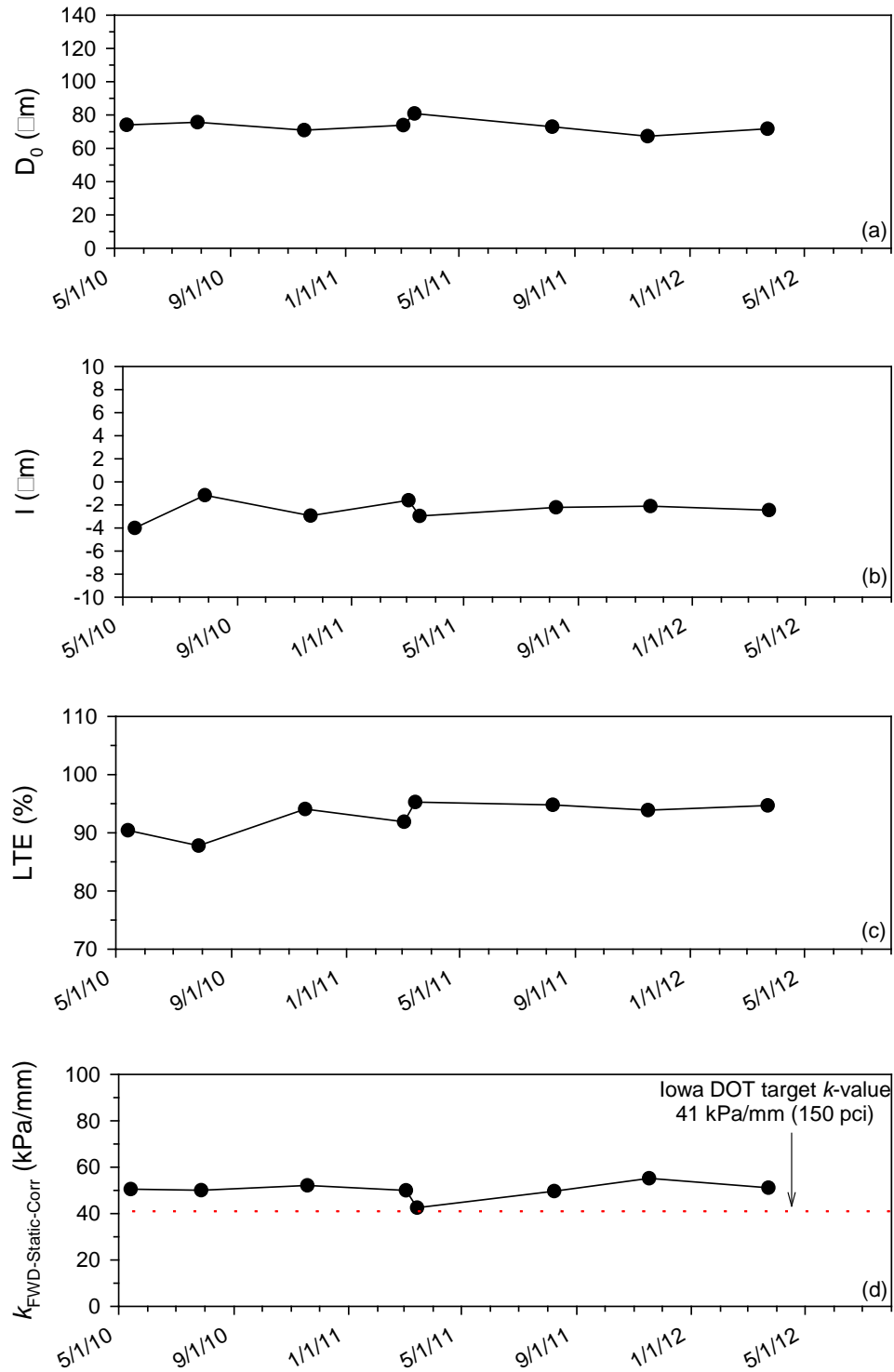


**Figure 40. Seasonal FWD test results of US 30 WB near MP 154.85, Nevada (Nevada east)**



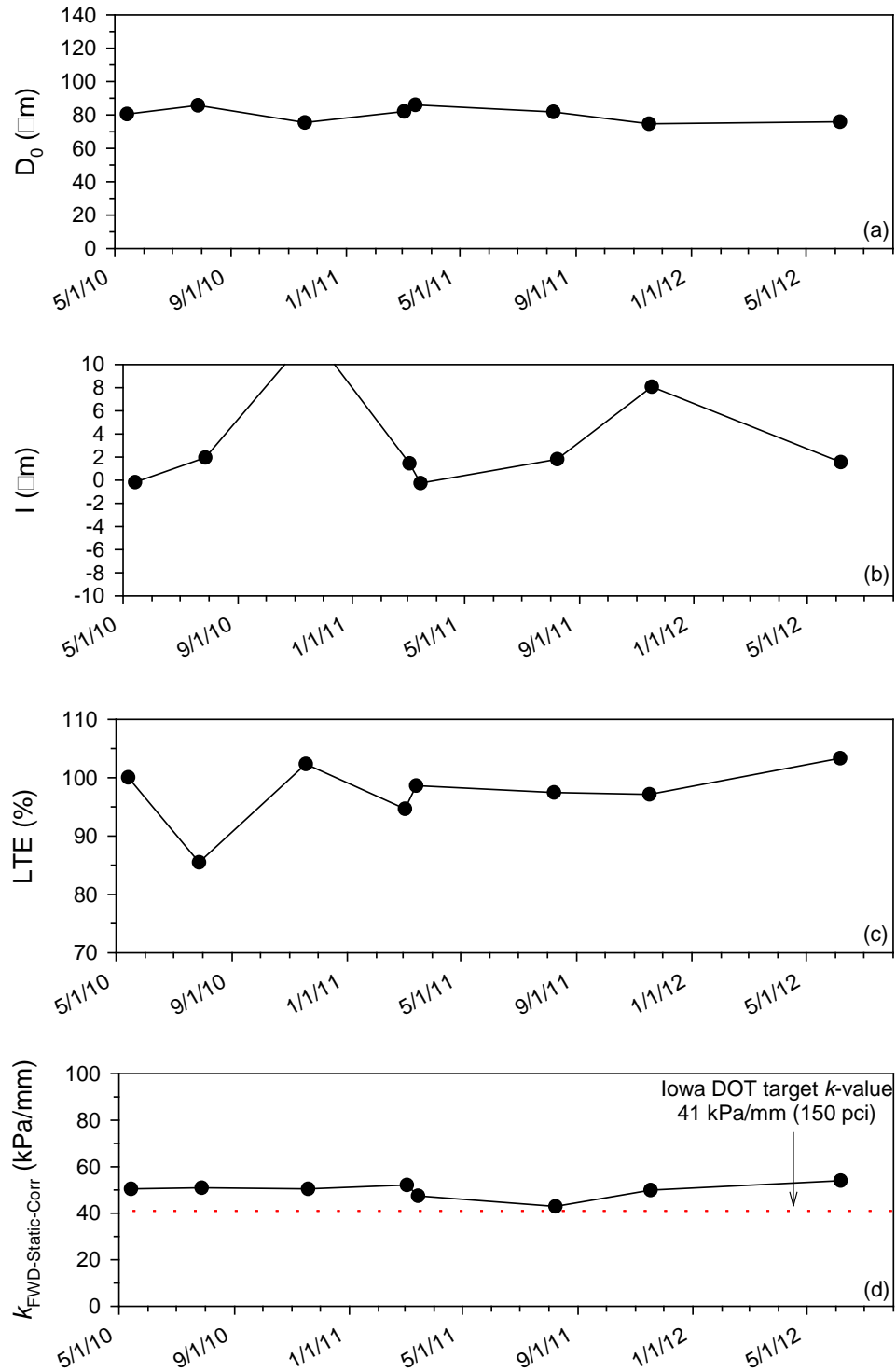


**Figure 41. Seasonal FWD test results of US 30 EB near MP 161.35, Nevada (Nevada west)**

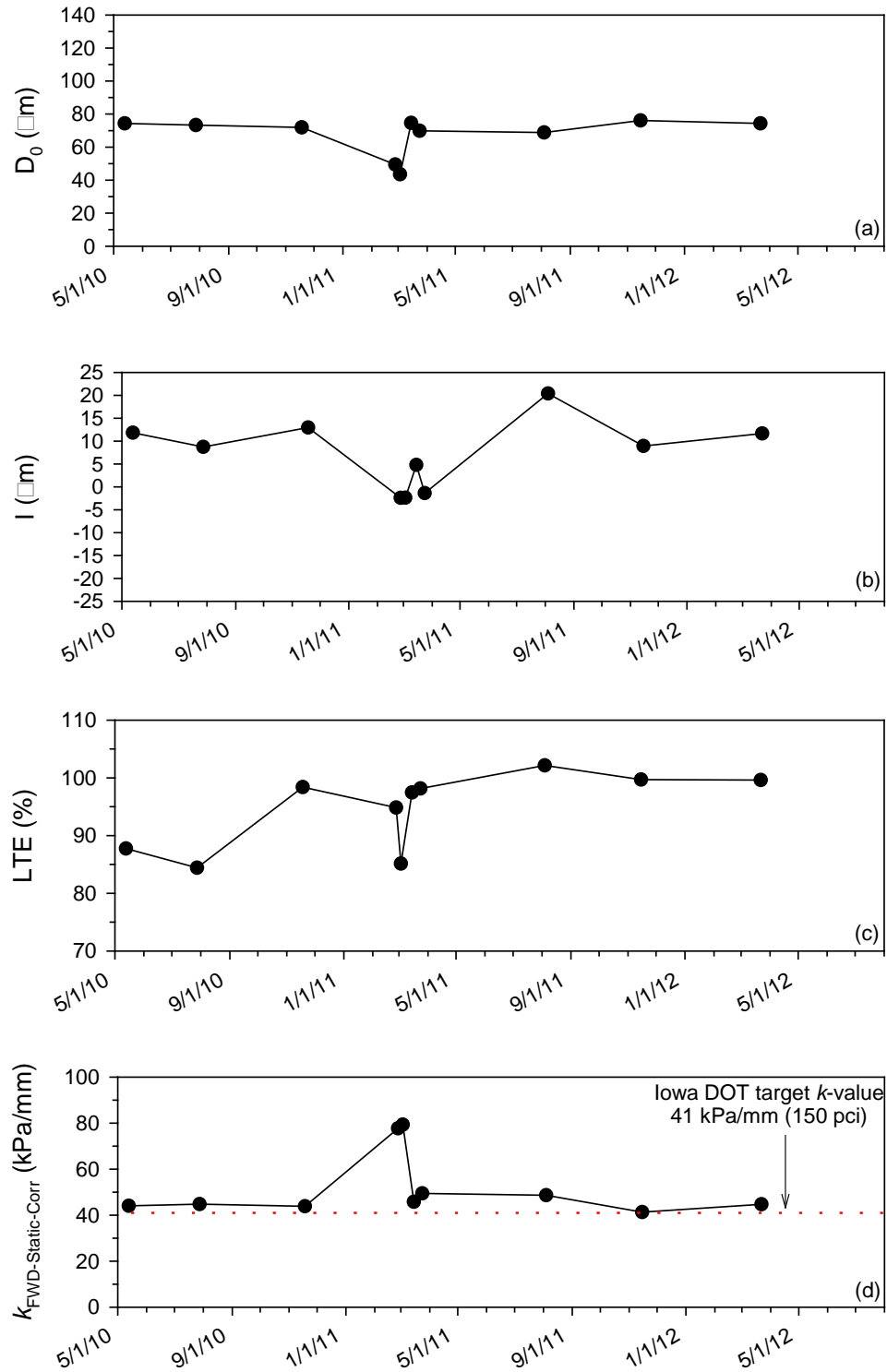


**Figure 42. Seasonal FWD test results of US 218 SB near MP 214.05, Plainfield**

## APPENDIX C: DCP TEST RESULTS

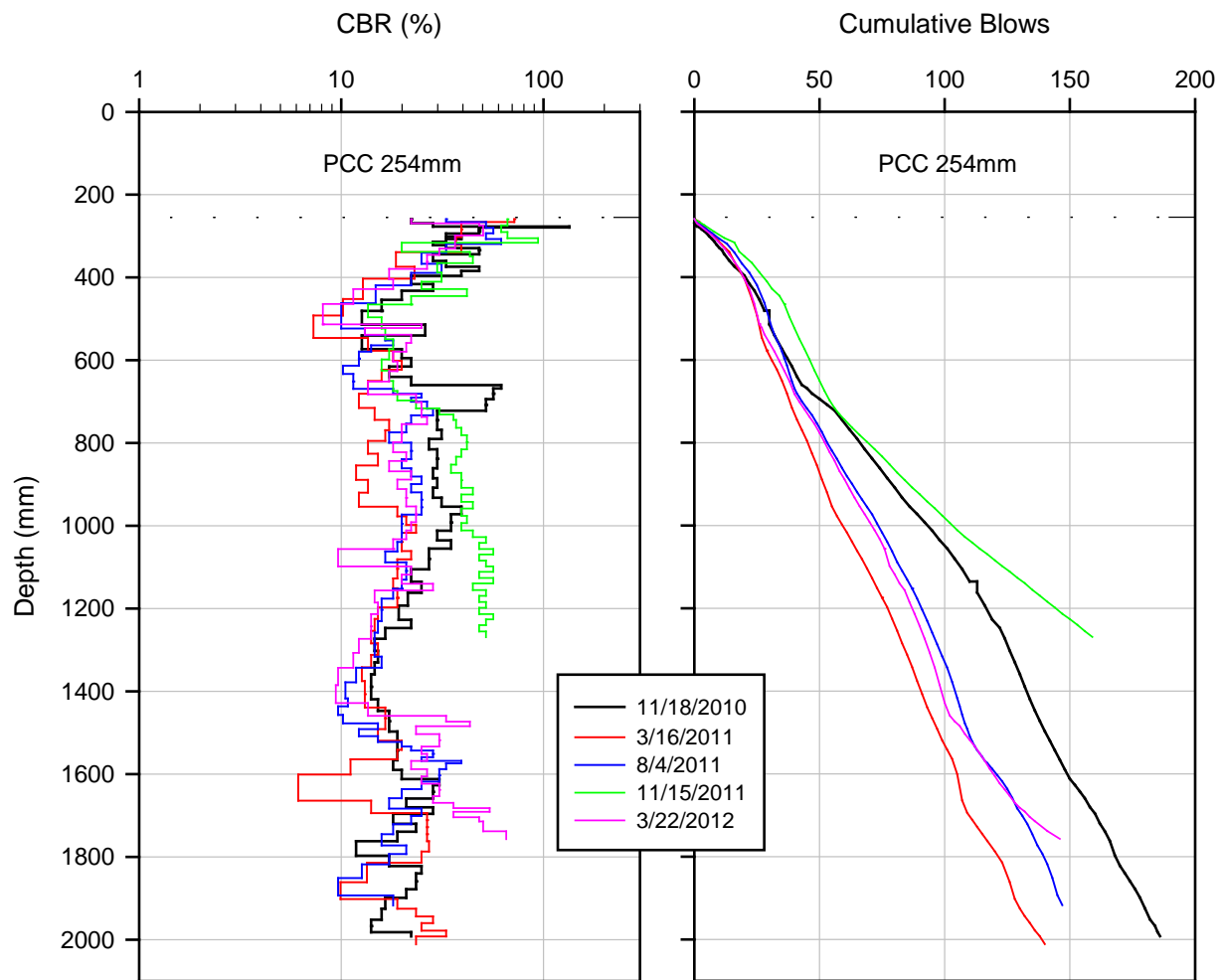
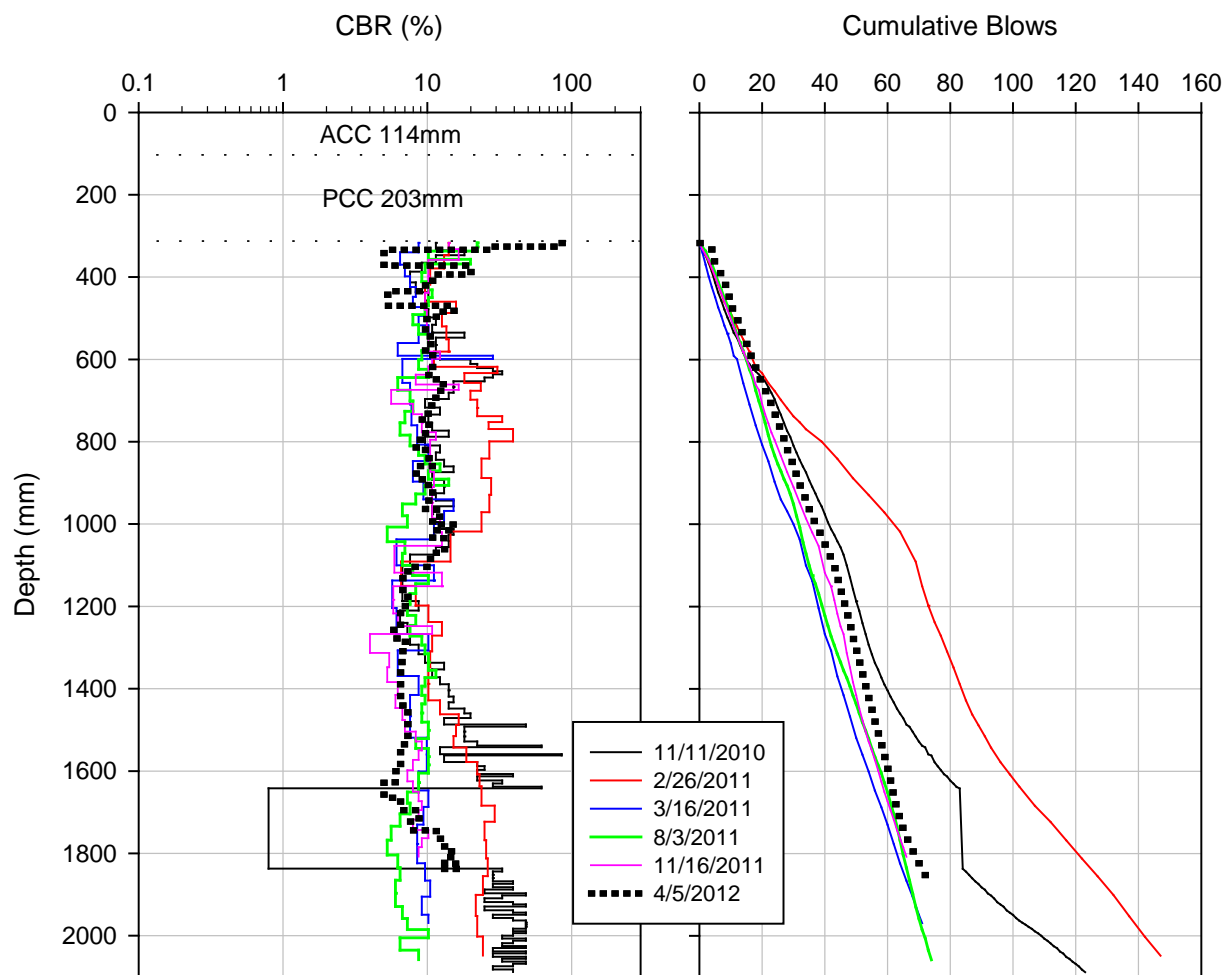
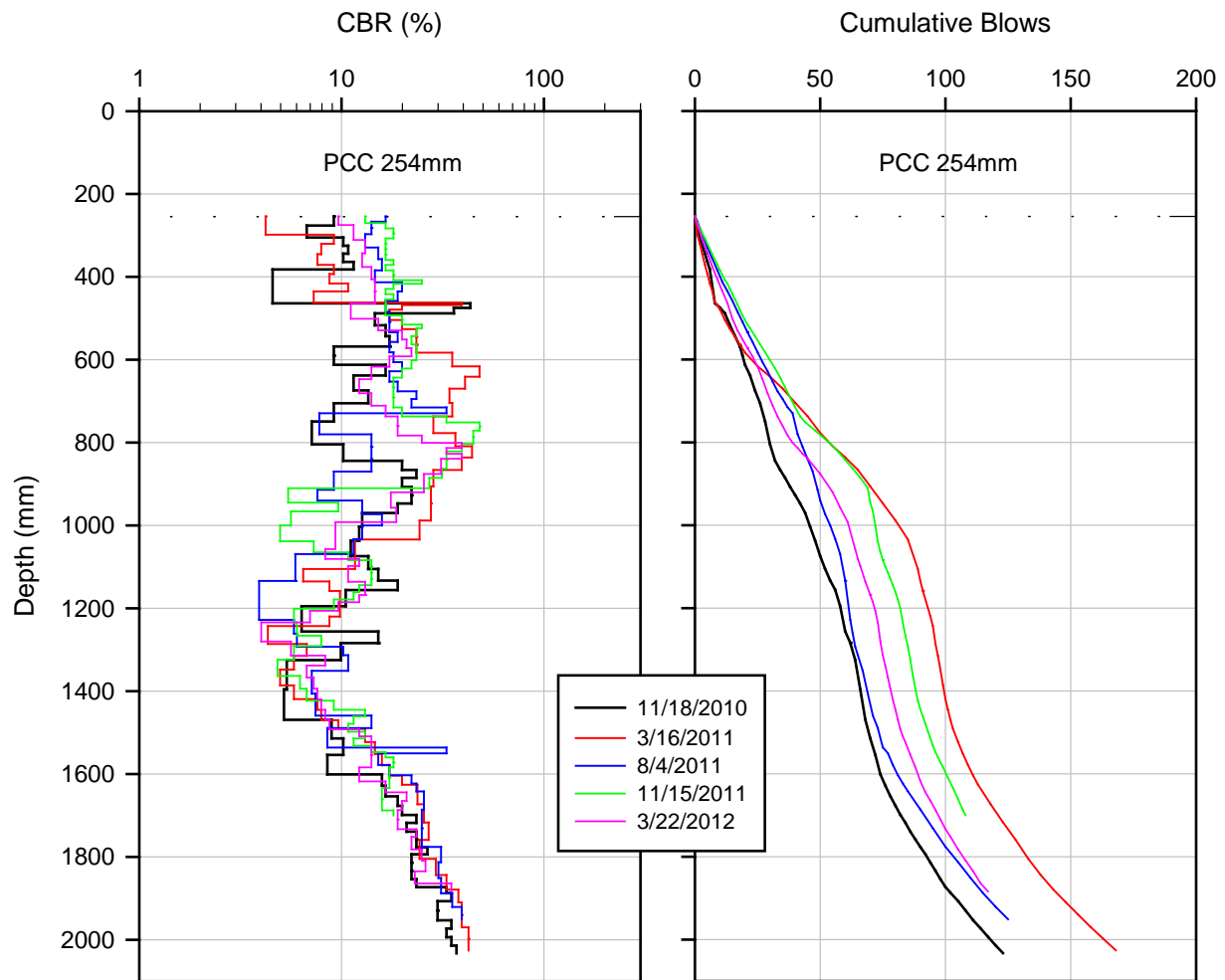


Figure 43. DCP-CBR profiles of US 20 WB near MP 18.5, Fort Dodge



**Figure 44. DCP-CBR profiles of US 59 NB near MP 95.0, Denison**



**Figure 45. DCP-CBR profiles of US 20 EB near MP 18.5, Moville**

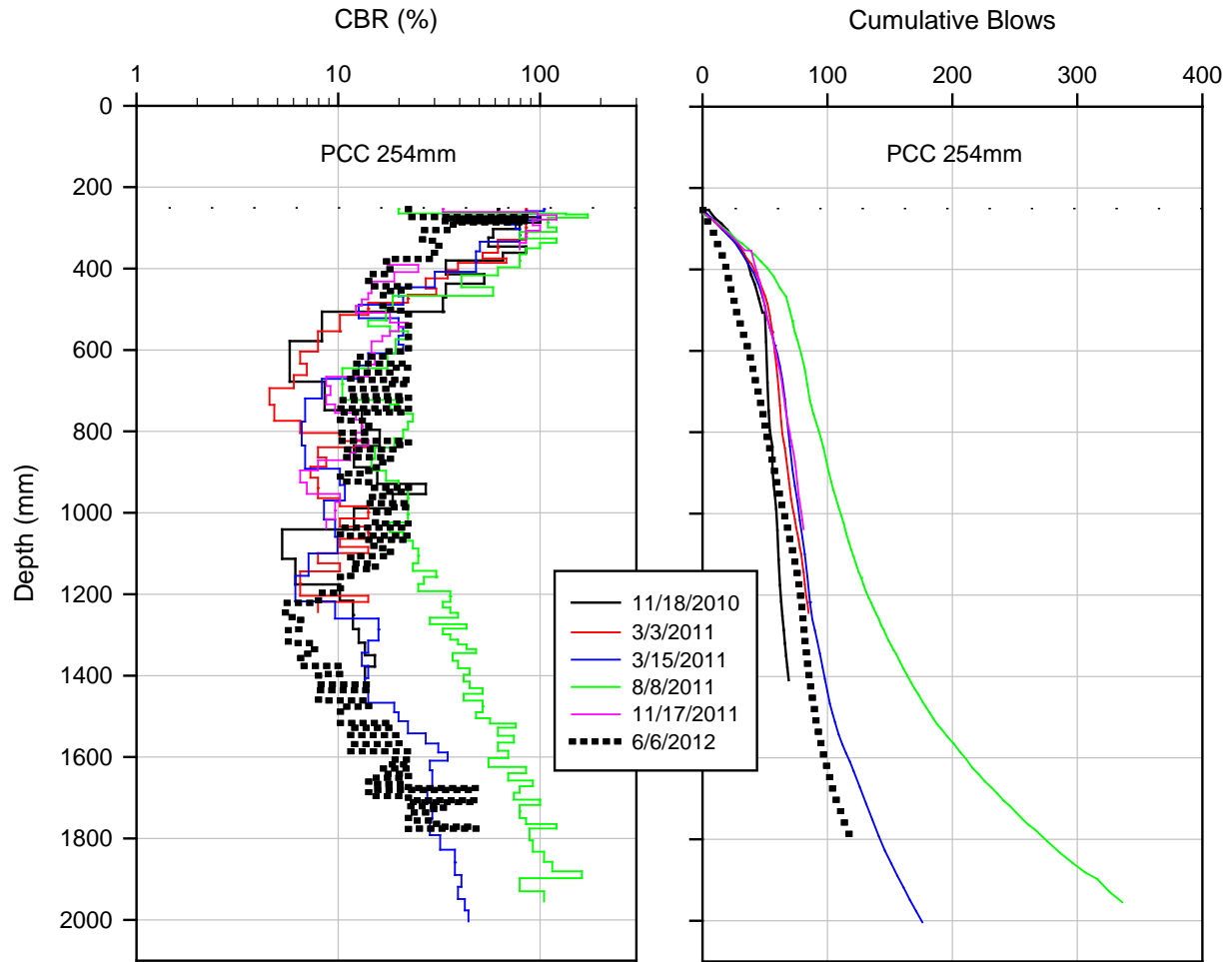


**Figure 46. DCP-CBR profiles of US 30 WB near MP 154.85, Nevada (Nevada east)**

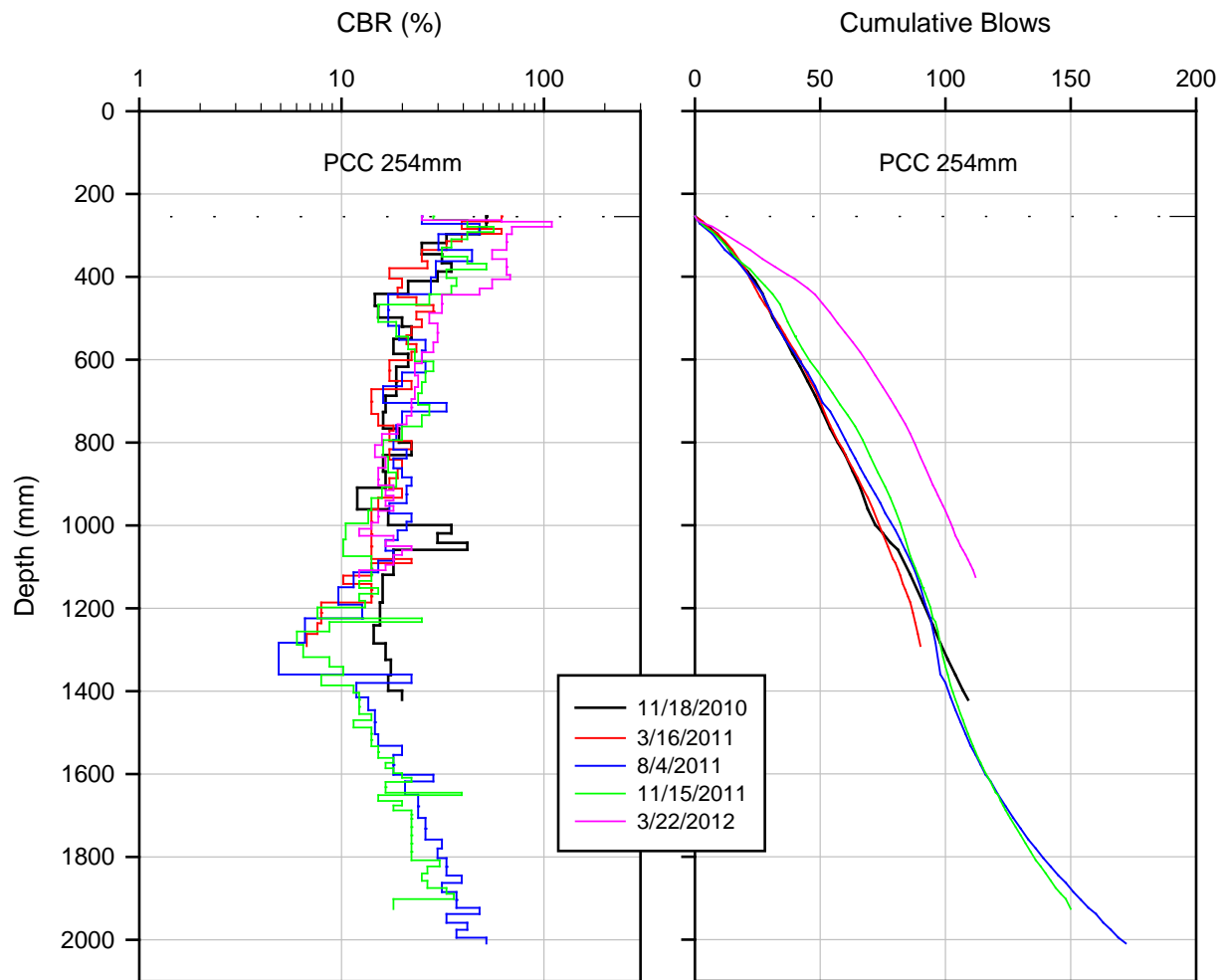


**Figure 47. DCP-CBR profiles of US 30 EB near MP 161.35, Nevada (Nevada west)**

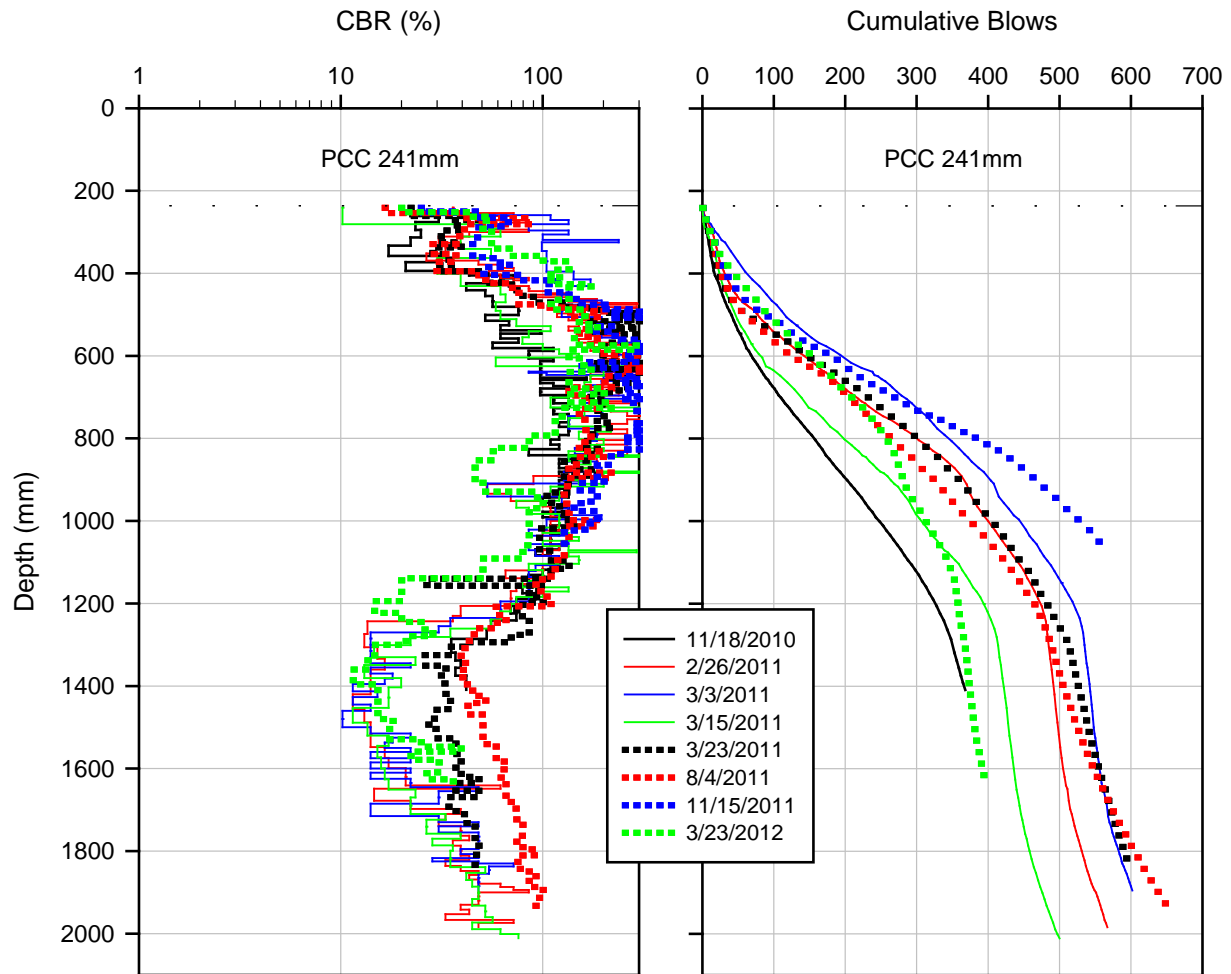


**Figure 48. DCP-CBR profiles of US 218 SB near MP 214.05, Plainfield**



## APPENDIX D: PICTURES FROM EACH TEST SITE



**Figure 49. US 20 WB near MP 18.5, Fort Dodge on 02/24/2011**



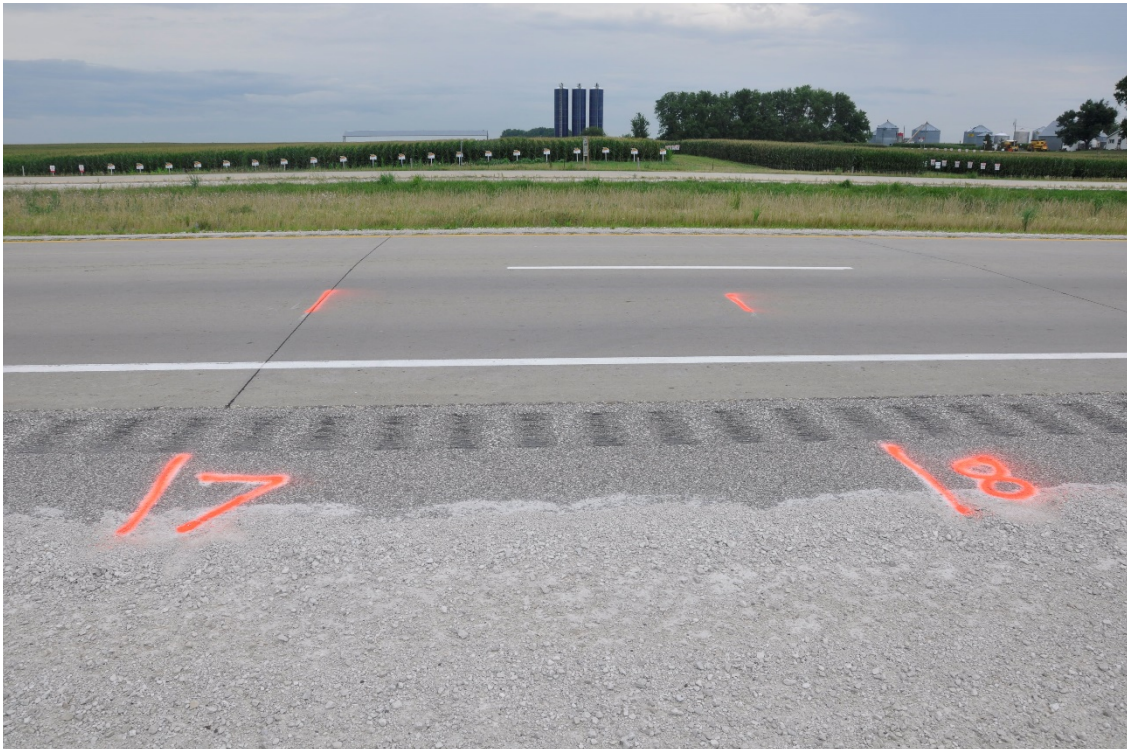


**Figure 50. US 20 WB near MP 18.5, Fort Dodge on 08/04/2011**





**Figure 51. US 20 WB near MP 18.5, Fort Dodge on 11/15/2011**





**Figure 52. US 59 NB near MP 95.0, Denison on 02/24/2011**





**Figure 53. US 59 NB near MP 95.0, Denison on 08/03/2011**





**Figure 54. US 59 NB near MP 95.0, Denison on 11/16/2011**





**Figure 55. US 20 EB near MP 18.5, Merville on 02/24/2011**





**Figure 56. US 20 EB near MP 18.5, Merville on 08/03/2011**





**Figure 57. US 20 EB near MP 18.5, Merville on 11/16/2011**





**Figure 58. US 30 WB near MP 154.85, Nevada (Nevada east) on 03/03/2011**





**Figure 59. US 30 WB near MP 154.85, Nevada (Nevada east) on 08/08/2011**





**Figure 60. US 30 WB near MP 154.85, Nevada (Nevada east) on 11/17/2011**





**Figure 61. US 30 EB near MP 161.35, Nevada (Nevada west) on 03/03/2011**





**Figure 62. US 30 EB near MP 161.35, Nevada (Nevada west) on 08/08/2011**





**Figure 63. US 30 EB near MP 161.35, Nevada (Nevada west) on 11/17/2011**





**Figure 64. US 218 SB near MP 214.05, Plainfield on 02/26/2011**





**Figure 65. US 218 SB near MP 214.05, Plainfield on 08/04/2011**





**Figure 66. US 218 SB near MP 214.05, Plainfield on 11/15/2011**